STUDIES OF MATRIX-ISOLATION SPECTRA IN SOLID HYDROGEN

Thesis by

Charles C. Runyan

In Partial Fulfillment of the Requirements

For the Degree of

Master of Science

California Institute of Technology

Pasadena, California

1972

(Submitted June 5, 1972)

ABSTRACT

Studies into the spectral features produced by atomic and molecular systems isolated in solid hydrogen have been undertaken to elucidate the nature of the interaction between the isolated species and the surrounding matrix. The absorption properties of matrix-isolated calcium are investigated to seek an understanding of the diffuse characteristics of absorption spectra perceived in stellar radiation that traverses interstellar dust clouds. The fine structural features of the $\tilde{A}^1B_{2u} \leftarrow \tilde{X}^1A_{1g}$ transition of benzene isolated in hydrogen are examined for their bearing on the extremely sharp lines exhibited by benzene in all light matrices.

The impure hydrogen samples are prepared for absorption investigations by depositing hydrogen and calcium or benzene onto a window cooled to $2^{\circ}K$. Besides the spectra of the above two systems isolated in hydrogen, the absorption signals of benzene in solid deuterium and of perdeuterobenzene in both solid hydrogen and solid deuterium are also presented. Furthermore, changes in the benzene fine structure that result from the reduction of the ortho/para ratio of the solid hydrogen medium are provided.

Because these studies have not been carried to completion, extensive detail in experimental procedures is supplied and

a brief analysis of the shifts and shapes of the observed absorption lines offers thoughts for further research.

TABLE OF CONTENTS

1. INTRODUCTION

The technique of isolating molecules in low-temperature matrices which are transparent to radiation in the infra-red, visible and near ultraviolet regions has become a standard tool of most optical spectroscopic laboratories since the early 1960's. Among the problems in chemistry for which this technique has been put to use have been the examination of the structure of short-lived molecular systems, such as free radicals or high-temperature molecules, and the identification of chemical intermediates to elucidate reaction mechanisms.

However, comparison of the spectra of an atom or molecule in a free state and in a matrix-isolation situation reveals significant differences in spectral line positions and shapes. Accounting for the spectral changes from the free case has been difficult and at the present time many problems remain in the analyses of matrix-isolated spectra. Yet it is important that an understanding of these spectral perturbations be found, as such an understanding would enable chemists to determine the unperturbed properties of molecular systems that would normally not exist in a free condition.

The research efforts to be described are concerned with atomic and molecular systems isolated in solid hydrogen. The problems of interest associated with this

particular solvent medium are listed below.

Outside of a cryogenic laboratory the existence of solid hydrogen is restricted to interstellar domains, as in dust particles or planetary mantles. This region of space is of great interest to astrochemists at the present time, and a spectroscopic study of impurities in solid hydrogen might be pertinent to a determination of the chemical make-up of interstellar dust particles. The spectra of such preparations might correlate with absorption features perceived in the spectral profile of stellar radiation that has traversed and interacted with clouds of dust particles.

Another interesting facet of molecular systems isolated in hydrogen matrices is the resulting fine structure characterizing the absorption spectra of benzene for the transition to the lowest-excited singlet state ($\tilde{A}\,^1B_{2u}$). The uniformity of intensity, the strong contrast, and the fineness of this structure has so far defied analysis. But since much of the difficulty in analyzing spectra of matrix-isolated molecules lies in the scarcity of information, a molecular system that offers additional data in the form of fine structure increases the possibilities of a successful rigorous analysis. Such analyses have been in short supply to date.

2. EXPERIMENTAL APPARATUS

Basic to all the experiments involving the generation of impure solid hydrogen samples is an apparatus consisting of two parts, a vacuum manifold in which hydrogen gas and the atomic or molecular impurity are mixed and a deposition chamber in which the gaseous mixture can condense out on an optically-transparent cold-finger. Much of this apparatus was designed and built by Mr. R. P. Frosch and is described in the gentleman's Ph.D. thesis.[1] Those components that have remained intact will be duly noted and the modifications will now be described in detail.

The entire system for generating hydrogen matrices is represented in block form in Figure 2-1. This diagram provides an overall perspective for use in the following discussions of individual system components.

The entire system is mounted upon a portable table of welded steel construction. No modifications of the table were made from the original design reported by Mr. Frosch.[1]

Vacuum Manifold

The vacuum manifold for solvent and solute mixing has been completely rebuilt, although the principles for generating mixtures of definite proportions are the same as described by Mr. Frosch. The following description of the manifold will refer to the illustrations in Figures 2-2 and 2-3. It is mainly constructed of Pyrex glass

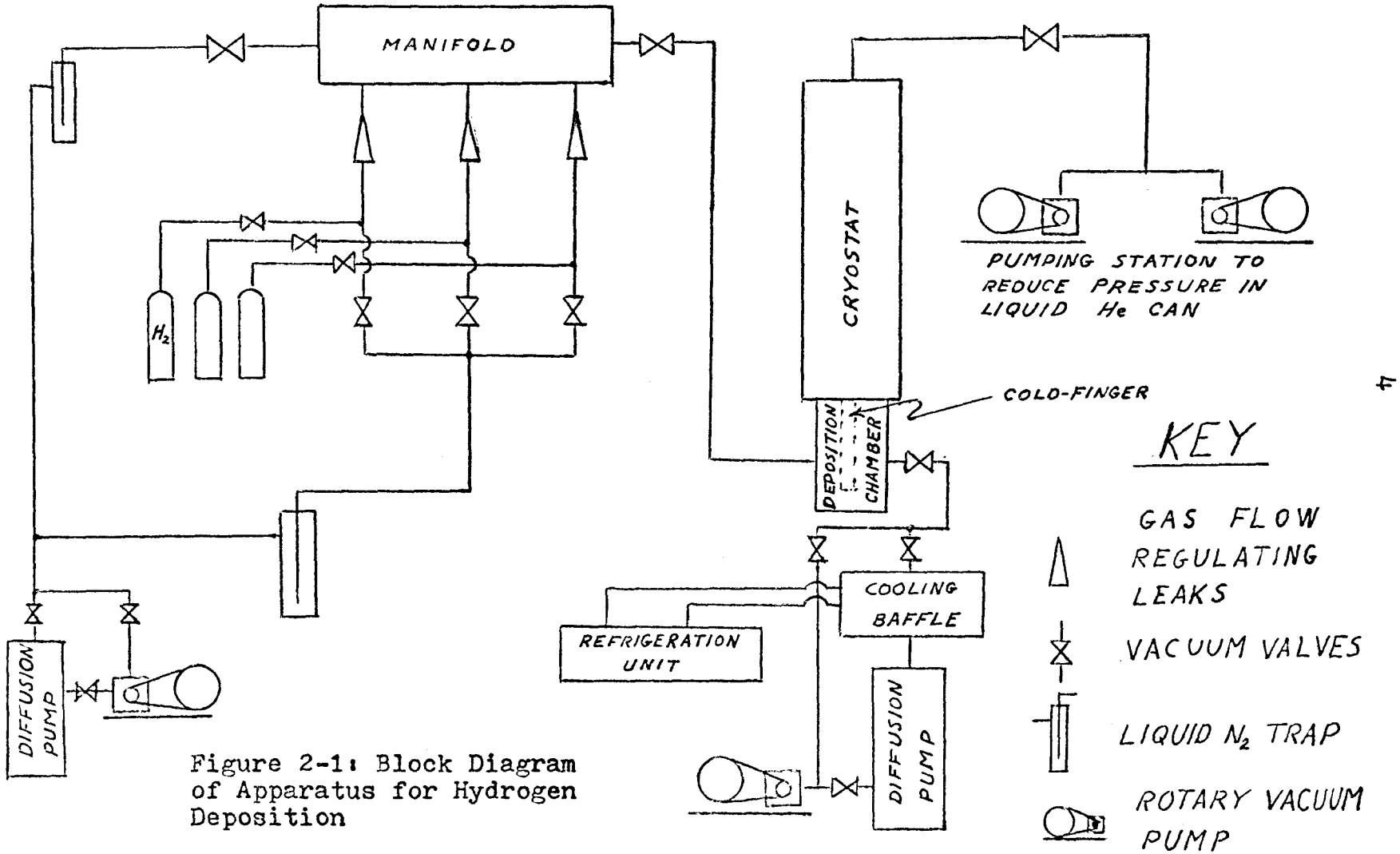

Figure 2-1: Block Diagram of Apparatus for Hydrogen Deposition

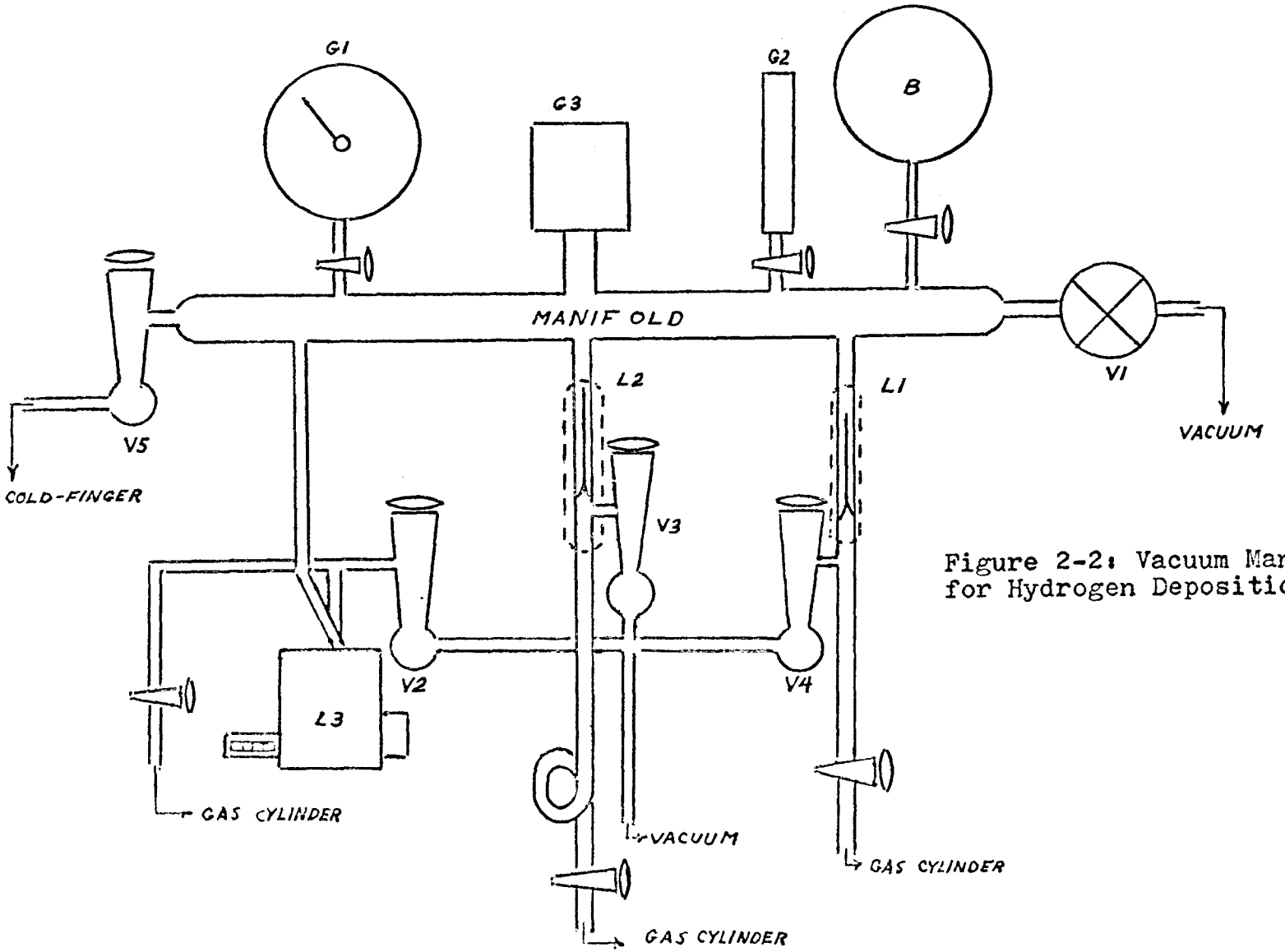

Figure 2-2: Vacuum Manifold for Hydrogen Depositions

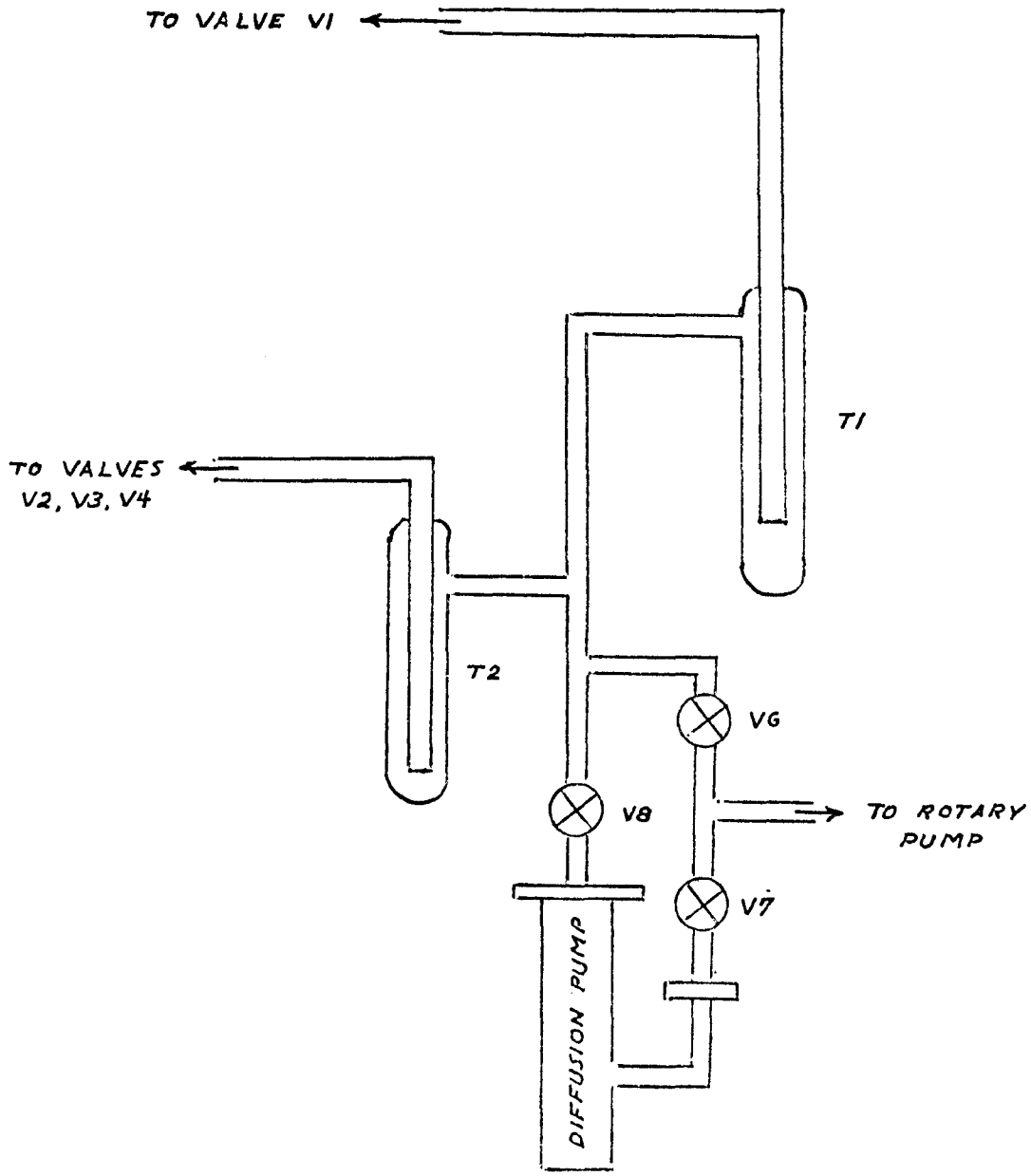

Figure 2-3: Pumping Station for Vacuum Manifold

tubing. Where glass-to-metal junctions are required, Pyrex glass-to-kovar metal seals are used. All stopcocks depicted in Figure 2-2 are lubricated with high-vacuum greases, specifically Apiezon L or M greases for their good lubricating and low-vapor-pressure properties as well as their ease in removal from glassware.

The manifold, a 50-cm. length of 25-mm. glass tubing, is connected to the vacuum pump through the valves marked in Figure 2-2 as V1, V2, V3 and V4. Valve V1 is a Kerotest two-way line valve with a nylon seat. The stopcocks V2, V3 and V4 are used to evacuate more rapidly the volume behind the flow rate leaks L1, L2 and L3. To evacuate this volume by pumping gas through the leaks would be painstakingly slow.

The stopcock valve V5 separates the manifold from the deposition chamber in order that either system can be evacuated or modified without affecting the other. It is opened only during an experiment when a gas mixture in the manifold is to be condensed out on the cold-finger.

In Figure 2-3 is an illustration of the pumping station for the manifold. The mechanical pump used to initially reduce the manifold pressure to a few mm. Hg and to back up the diffusion pump is a 140 l./min. Welch Duo-Seal two-stage, rotary vacuum pump. It is directly connected to the manifold through Kerotest

valves V1 and V6.

The manifold pressure can be reduced to about 10^{-5}mm. Hg by operation of the diffusion pump, which is connected to the rotary pump through the Kerotest valve V7 and to the manifold through Kerotest valves V1 and V8. A CVC PMC-115, 2-inch, oil diffusion pump is used.

In order to keep pumping oil from reaching the manifold during evacuation, two Pyrex traps maintained at liquid nitrogen temperatures are situated between the manifold and pumping station. They are denoted as T1 and T2 in Figure 2-3.

For monitering manifold pressure three pressure gauges, denoted as G1, G2 and G3 in Figure 2-2, are connected directly to the manifold. Gauge G1 is a 0-40mm. Hg vacuum pressure gauge, used primarily in measurements of manifold volume and rates of gas flow through the leaks into the manifold. Gauge G2 is a NRC Type 105 thermocouple gauge which is also used for leak flow rate measurements as well as monitoring manifold pressures of a few microns Hg. And gauge G3 is a NRC Type 518 ionization guage, used to determine the ultimate vacuum attainable with the diffusion pump.* Both gauges G1 and G2 are isolated from the manifold

*The ionization gauge is not essential to the operation of the manifold. A thermocouple gauge would detect any significant vacuum leaks into the manifold.

by stopcock valves to prevent all but chemically inert gases from entering.

The 2-liter glass bulb, denoted as B in Figure 2-2, is used in the determination of the manifold volume by a method to be described in Section 3. By measurement of the amount of water required to fill the bulb, the volume above the stopcock is found to be 2040 ml. with a 1% confidence limit.

The critical elements to the manifold function of mixing gases in desired proportions are the gas flow controlling leaks, designed to operate with a back-pressure of one atmosphere. The fixed leaks L1 and L2 are fashioned out of Pyrex 0.75-2.0 mm. i.d. capillary tubing whose inner bore has been heated and constricted to a size that provides the desired gas flow rate. Leak L3 is a Granville-Phillips Series 9100 all-metal variable leak with a leak capability of 10^{-8} - 10^{3} ml. STP per minute.

Each leak has a particular function in the operation of the manifold. Leak L1 is used solely for establishing a hydrogen gas flow rate of 1-3 ml. STP per minute, while leak L3 is provided to introduce into the manifold at a controlled rate gaseous material to furnish the solute of the solid hydrogen solution. To protect the metal seating surfaces, only non-corrosive gas flows are regulated by the variable leak. Consequently, leak L2 not

only offers a means to introduce additional material into the manifold but also makes available as solute material gases corrosive to metal surfaces. Both leaks L2 and L3 are downstream to the hydrogen leak L1 to insure that the solute gases mix with the hydrogen stream before exiting from the manifold.

A note should be made of the coil of Pyrex tubing situated behind leak L2 as indicated in Figure 2-2. Because the capillaries in fixed leaks such as L1 and L2 are very fine, any "dust" particles in the gas line may eventually be carried into the leak capillary with a resultant stoppage. The coil has been introduced as a remedy by eliminating a straight path from the gas line to the leak L2.

To introduce into the hydrogen flow solute material that exists in a condensed phase at room temperature and pressure, an alternate method exists to one in which leaks would be utilized. It involves directing the hydrogen flow through a reduced-temperature trap containing the material, as illustrated below. As the flow plays over the surface of the condensed material, a mixture results with a concentration make-up approximated by the ratio of hydrogen manifold pressure to the vapor pressure of the guest material at the reduced temperature of the trap. This ratio is larger than actual gas mixture proportions since some entrainment by the hydrogen flow of the solute occurs.

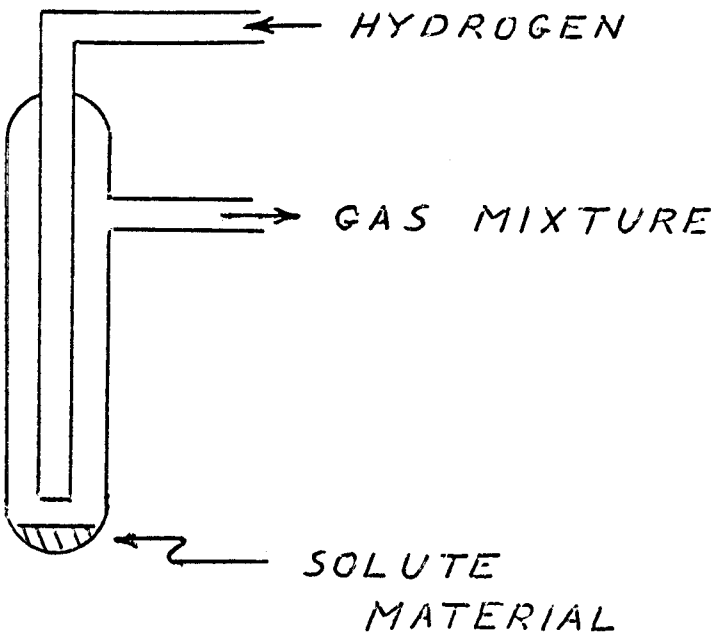

Flow Line

Since a liquid-helium-cooled cold-finger is necessary to freeze hydrogen gas, a vacuum condition must be maintained in the deposition chamber to prevent intolerable loss rates of liquid helium due to gases acting as convection- or conduction-type heat sources.[2] As a result the steady-state pressure of the gas mixture must be reduced from the manifold value of a few mm. Hg to a value roughly 10^{-4} mm. Hg or less within the deposition chamber. This is achieved by pumping on the manifold through valve V5 (Figure 2-2) with the pumping station behind the deposition chamber. Large reductions in gas density can be achieved along a transfer line for gas flow at points at which a large decrease in the cross-sectional area of the transfer line occurs. Such

is the function of the flow line, depicted in Figure 2-4, for transport of the gas mixture from the manifold to the deposition chamber.

The first constriction upon the gas flow occurs at valve V5 at which the diameter of the flow line decreases from that of the manifold to the i.d. of 7-mm. Pyrex tubing. Just beyond the O-ring junction the flow line consists of capillary tubing which further restricts the gas flow with a reduction in i.d. to one mm. The final barrier to gas flow occurs at the partition between the two chambers denoted in Figure 4 as the "spray" and "plasma" chambers. Gas entering the "plasma" chamber, with a typical dimension of 10 mm., can pass on to the deposition chamber only by passing through a 0.5-mm. diameter hole in the partition. Now the gas density of the flow in the deposition chamber is sufficiently reduced to provide good thermal insulation for the liquid-helium-cooled surfaces.

The "spray" chamber derives its name from the description of the gas flow beyond the 0.5-mm. diameter aperture. Gas exiting from a chamber through a small hole in the chamber wall will exit in the form of a spray. This is to insure that the solid hydrogen film that forms upon the cold-finger is of uniform thickness.

In addition to eliminating heat losses for liquid

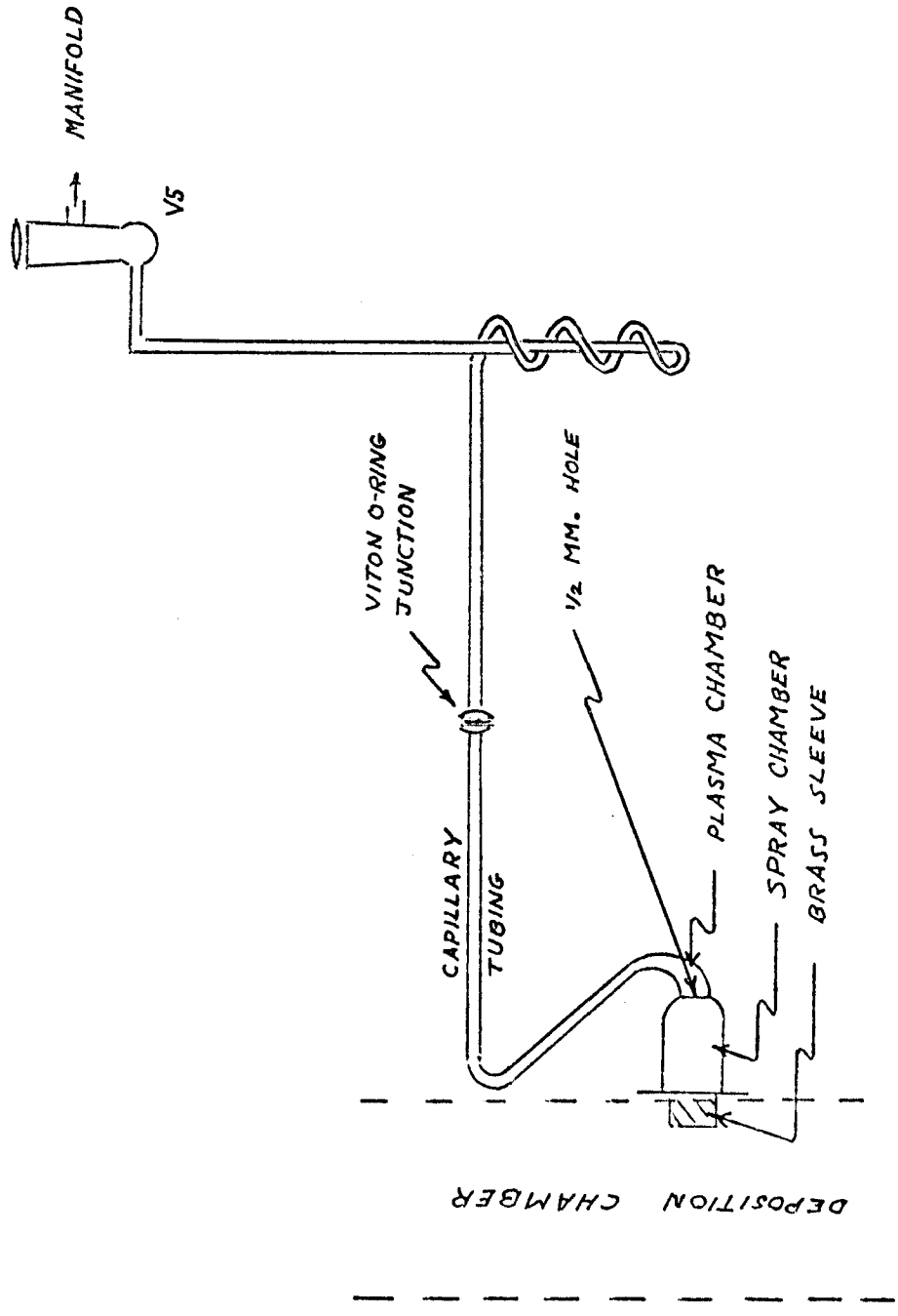

Figure 2-4: Hydrogen Flow Line Between Vacuum Manifold and Deposition Chamber

helium, an additional factor dictates that the density of gas be kept low within the "spray" and deposition chambers. It may be of interest to isolate in the hydrogen matrix short-lived atomic or molecular systems, which shall be collectively termed as radicals. If radicals are not formed as dissociation products of stable molecular systems isolated in solid hydrogen prior to dissociation, then it is desirable that the radical mean free path is comparable to the distance between the site of generation and the cold-finger. With a gas density corresponding to a steady-state pressure of 10^{-4} mm. Hg the mean free path is roughly 10 cm.[3], i.e., a distance on the order of that existing between the "spray" chamber and the cold-finger.

The "plasma" chamber can serve as the point of generation of transient molecular and atomic systems if an electrical discharge in the gas mixture can be initiated within the chamber. With the flow line geometry depicted in Figure 2-4, a convenient method for sustaining a discharge is by situating a source of microwaves immediately outside the chamber. No metal electrodes need to be built into the chamber, as in low-frequency discharges, on which may readily take place reactions involving the radicals. Initiation of the discharge is easily managed by providing a source of electrons to the

chamber as with a tesla coil. It is observed that the manifold pressure has to drop to a few mm. Hg before initiation of a discharge in the "plasma" chamber will occur.

One precaution to observe (besides not touching the antenna once microwave generation begins) is to cool the chamber walls heated by dielectric losses and heat transfer from the neighboring plasma. A cooling medium, such as an air blast, transparent to microwave energy may be used.[4] In addition, unless 1-2 mm. distance is maintained between the center of the microwave antenna and the chamber wall under conditions of air cooling, a hole will form in the wall with subsequent loss of vacuum.

In the spray effusing from the "plasma" chamber will be a quantity of radicals that have not recombined before exiting. An unobstructed pathway now exists to the deposition surface. And, barring any reaction with solid hydrogen, isolation of these unstable particles in an inert environment is completed.

Short-lived substances generated in a discharge are necessarily derived from parent molecules in the manifold with a room temperature vapor pressure on the order of a few microns Hg or larger. For material with lower vapor pressures at room temperature the application

of heat becomes necessary to incorporate substances such as metal atoms or high-temperature molecules into the flow. With the present design of the flow line the source of high-temperature atoms or molecules should be in the "spray" chamber to assure a free path from the oven to the cold-finger. Otherwise, deposition on the walls or reaction with the hydrogen flow will occur.

Consequently the flow line between the deposition chamber and the O-ring junction can be removed to allow the insertion of a "spray" chamber housing an oven. The present system utilized an oven heated resistively mounted on electrical feedthroughs in the "spray" chamber wall. But oven "spray" chambers utilizing, for example, inductive heating or electron bombardment can be installed as well.

Deposition Chamber

The deposition chamber* is the same as that described by Mr. Frosch[1] with only the usage of the chamber ports in the generation of hydrogen matrices differing somewhat. Port B, as labelled by Mr. Frosch, is still the evacuation port, and in absorption studies the cold-finger is illuminated through port D and

*The deposition chamber is referred to as the base in Mr. Frosch's terminology.(1)

unabsorbed light is monitored through port F. Since no experiments have been conducted in the vacuum ultraviolet, the light source is external to the deposition chamber requiring the installation of a window at port D. (At the time of this writing, port D is covered with a quartz window while that across port F is of barium fluoride.) Vacuum sealing is accomplished by pressing the windows into Viton O-rings situated in grooves about the ports.

Port C has not been used for deposition purposes. It is directly connected to the external atmosphere through a bellows valve and has been used to open the chamber to the atmosphere.

Port E is used to admit deposition gases from the "spray" chamber. To make a vacuum seal, a brass sleeve to which is epoxied the spray chamber, as illustrated in Figure 2-4, rests against a Viton O-ring encircling the port aperture. The pressure differential between the evacuated chamber and external atmosphere insures a vacuum-tight connection.

Cold-Finger and Cryostat

The stainless steel cryostat and its pumping system are the same as those used by Mr. Frosch[1] in his matrix-isolation studies with only a few modifications necessary for hydrogen-deposition operations.

Nearly all the hydrogen introduced for deposition during an experiment is eventually pumped out by the CVC 4" oil diffusion pump backing up the deposition chamber. The hot oil must not be reactive to hydrogen gas, as a result, if optimum vacuum conditions are to be maintained. With an ester-type oil, such as Octoil, a light-colored waxy substance has been found to form in the diffusion pump after several hydrogen depositions with a consequent degradation of vacuum in the cryostat. Switching to a hydrocarbon-type oil, such as Convoil-20, has remedied this situation with no vacuum deterioration after roughly twenty separate hydrogen depositions.

At the temperature of the cold-finger during an experiment ($\sim 2^{\circ}$K.), mere water cooling of the 4" chevron baffle above the diffusion pump does not prevent diffusion-pump oil vapor from condensing onto the cold-finger. As a result, a refrigeration unit has been connected to the coolant ports of the baffle, reducing oil vapor backstreaming to negligible amounts.

Mention should be made of a periodically troublesome leak in the pumping system. It exists at the soldered junction of the vacuum line that bypasses the diffusion pump with the 4"-diameter stainless steel tubing that connects the two gate valves. Attempts at repair using Glyptal lacquer cement are successful for a period

of time. Its reappearance can probably be attributed to pressure cycling.

As hydrogen condensation at $4.2^{o}K.$, the normal boiling point of liquid helium, is an inefficient operation in the present deposition chamber, an alteration in cryostat operation is necessary for generation of hydrogen films. At this temperature the vapor pressure of solid hydrogen is between 10^{-6} and 10^{-7} mm. Hg with a desorption rate of $\sim 10^{20}$ mol $m^{-2}sec^{-1}$.(5) The desorption rate of hydrogen from the cold-finger could be larger by several orders of magnitude due to the incidence of thermal radiation through the windows and to the poor thermal conductivity of solid hydrogen that lies between the liquid helium bath and the outer surface of the hydrogen film. Since the deposition chamber is evacuated to $\sim 10^{-7}$ once the hydrogen flow has ceased, much of the desorbed hydrogen is not returned to the cold-finger. But it is desirable to retain all hydrogen molecules that strike the cold-finger in order that the solute concentration is maintained at the manifold value throughout the duration of the experiment. This condition approaches actuality if the cryostat temperature is reduced to $\sim 2^{o}K.$

A reduction in pressure above the surface of the liquid helium bath cools the refrigerant until the rate of heat removal in evacuation is equal to the rate of heat loading from outside the cryostat. With the utilization

of two 140 l./min. rotary vacuum pumps to pump on the liquid through the cover to the liquid helium cryostat cylinder, the temperature can be reduced to below the point (2.2°K.) at which the helium λ phase transition occurs. A 0-760 mm. Hg vacuum pressure gauge is used to monitor the reduction in pressure. It is important that the liquid helium container and evacuation line be vacuum-tight to prevent the introduction of air in the pumping process. Frozen air would possibly block passage of light through the cold-finger or block passage of helium vapor from the cryostat.

The cold-finger described by Mr. Frosch[1] has proven to be inadequate for hydrogen depositions. Indium seals about the sapphire windows constantly require renewal, as helium penetrates into the evacuated deposition chamber after only 2 or 3 hydrogen depositions. No error in indium seal installation is discernible. The leak possibly develops as the pressure within the cold-finger and liquid-helium cylinder repeatedly cycles between zero and atmosphere.

The incorporation into the cold-finger of Ceramaseal high-vacuum sapphire window assemblies has eliminated the occurrence of leaks. These window assemblies consist of 0.5"-diameter sapphire windows brazed into a nickel-iron alloy sleeve which is in turn brazed to a stainless steel adapter. The final configuration of the cold finger is

illustrated below. Note that the groove that lies on the outer edge of the circular face provides a thin wall between the sapphire window and the indicated welding site to diminish the flow of heat to the window during the welding operation. This reduces the chances of a window cracking or the vacuum seal degrading.

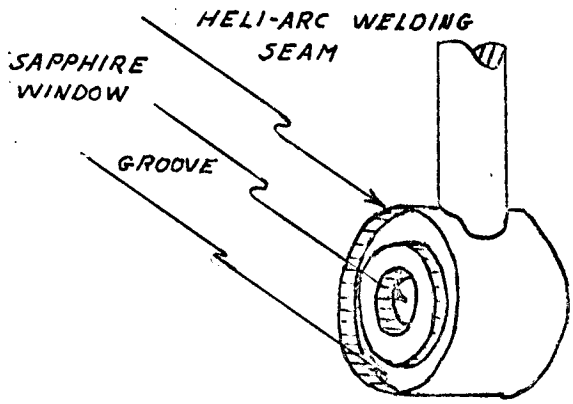

The completed stainless-steel cold-finger assembly is attached to the bottom of the cryostat liquid helium can with the illustrated flanged junction. Indium wire is used to provide the vacuum seal.

The final modification to the cryostat design pertains to the copper heat shield surrounding the cold-finger. Only two apertures are incorporated into the shield for the purposes of deposition and, after a 90^{o} rotation of the cold-finger in the deposition chamber, the passage of

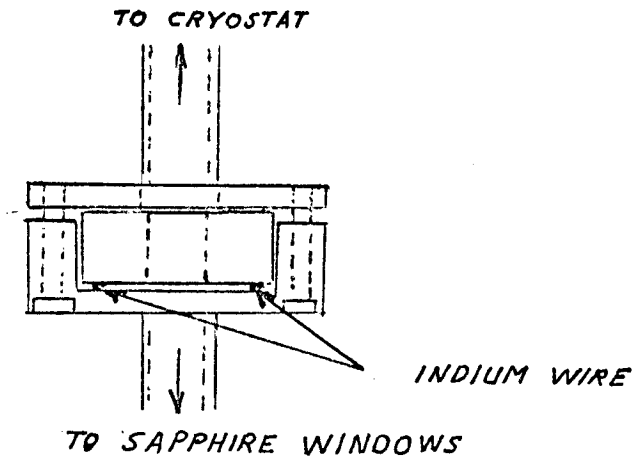

light in the illumination and detection of spectra. The aperture diameter has been reduced to 0.25" to lessen the amount of radiative heating through the shield apertures. Reduced radiation loading of the cold-finger is also achieved if the shield surface does not become oxidized since an order-of-magnitude increase of the surface emissivity results from oxidation.[2] It is then sensible to bring the pressure of the deposition chamber to atmosphere whenever necessary with an inert gas, such as helium. With diminished heat sources, lower temperatures and long lifetimes of the cryostat liquid helium supply under reduced pressure ($\sim$ 10 hours) are attained.

REFERENCES

1. R. P. Frosch, Ph.D. Thesis, Calif. Inst. of Tech., 1965.

2. G. K. White, Experimental Techniques in Low-Temperature Physics, Oxford Univ. Press, 1959.

3. S. Dushman, Scientific Foundations of Vacuum Technique, Wiley & Sons, 1962.

4. A. M. Bass, H. P. Broida, Eds., Formation and Trapping of Free Radicals, Academic Press, 1960.

5. V. C. Reddish, Nature Physical Science 231, 193 (1971).

3. TYPICAL EXPERIMENTAL PROCEDURE

Prior to any experiments requiring hydrogen depositions, it is necessary to install leaks into the manifold providing the desired flow rates. Knowledge is required of the manifold volume between valves V1 and V5 (Figure 2-2) before rates are measured, however. A sufficiently accurate value may be obtained by leaking hydrogen into the evacuated manifold exclusive of the evacuated 2-liter bulb B, allowing the pressure to reach a steady-state, and monitoring the pressure drop when the bulb is opened to the manifold.

The rate of gas flow through a leak into an evacuated manifold is now monitored with the resulting pressure rise. If the thermocouple gauge G2 is used*, corrections to the pressure readings according to the particular gaseous material monitored should be considered. (The temperature of a heated filament in the thermocouple gauge depends on the heat conducting capability of the surrounding gas at a given pressure.) All rate measurements are performed with a pressure differential of one atmosphere across the leak.

The flow rate is small enough to satisfy perfect gas conditions. With knowledge of the manifold volume,

*Whatever gauge is used, its volume is included in the manifold volume determination.

the pressure rise is related to the rate of material introduction into the manifold. Conventionally the flow rate is recorded as the volume increase at STP conditions per unit of time.

In preparation for generation of solid hydrogen matrices, the system of manifold, gas lines, flow line and deposition chamber is to be evacuated. All sources of contaminating vapors, such as material soluble in stopcock grease, are eliminated. If the impurity of interest is derived from an oven-heated material, the oven must be loaded before evacuation of the deposition chamber and flow line. A check of the operation of cooling lines to the diffusion pumps and chevron baffle are made and the traps in the pumping lines to the manifold are immersed in liquid nitrogen. After the pressure is initially reduced with the mechanical pumps, the diffusion pumps are warmed up, the system now isolated from the outgassing diffusion pump oil. Once the system is opened up to the diffusion pumps, evacuation is allowed to continue for at least twelve hours

At this stage the refrigerant cans of the cryostat are readied for cooling. Water must be removed from the liquid nitrogen compartment. Otherwise the compartment will rupture from expansion of water in freezing. Methanol is added to mix with the water, the mixture then being

drawn out with an aspirator. The liquid helium can including the cold-finger must likewise be dried. Two methods that have been used are to purge with dry nitrogen or to evacuate with the liquid helium pumping system. Care must be taken with the latter method to insure that the deposition chamber is under vacuum preventing the thin-walled helium can from buckling.

When the pressure in the deposition chamber has dropped to 10^{-6} - 10^{-5} mm. Hg, the cryostat is cooled down. Liquid nitrogen is added to the outer cryostat can and, in the meantime, the inner can for liquid helium is being slowly purged with dry helium gas. This prevents the condensation of vapors while providing a thermal connection between the inner can and liquid nitrogen reservoir in the outer can.

With the cryostat temperature at 77°K., the pressure eventually drops below 10^{-6} mm. Hg. At this time liquid helium is transferred from a storage dewar to the inner cryostat can. A successful transfer technique, which has been used with this system, is presented in G. K. White's text.[2] All air is purged from the transfer line with helium gas prior to its insertion into the dewar and the cryostat to prevent formation of a solid air plug. Sleeves of rubber tubing attached to the transfer line slip over the mouths of the dewar and cryostat to reduce

frost formation in the necks of the containers and to allow the rise of pressure in the storage dewar which effects the transfer. This overpressure is sustained by squeezing a rubber bladder directly connected to the liquid helium vessel of the storage dewar. Helium vapors during transfer exit to the atmosphere from the top of the cryostat.

Use of a bladder in the initial stages of the transfer operation is recommended to minimize the amount of liquid helium consumed to cool the helium cryostat can to $4^{o}K$. A small overpressure is produced to allow evaporated liquid helium to slowly exit from the cryostat, deriving most efficient use of the cooling capabilities of cool helium vapors. Consequently it is necessary that the transfer line extends to the bottom of the cold-finger so that the entire helium can is cooled by the rising vapors. When the cryostat temperature is estimated to be near $4^{o}K.$, the overpressure is maintained at a constant one p.s.i. by connecting the dewar to a helium gas cylinder. The transfer shortly begins and one liter of liquid helium is obtained in a period of $\frac{1}{2}$ - 1 minute. With this method only two liters of liquid helium should be consumed in the transfer.

Upon completion of transfer the pressure reduction in the liquid helium can is begun. The initial pumping

rate is kept low to minimize the loss of helium while its vapor pressure is high. As the pressure drops the pumping rate is kept at a given level by steadily opening the valve. Forty-five minutes is usually required to reach the helium λ point at which time hydrogen deposition commenses.

Meanwhile the manifold has been isolated from its pumps when its pressure is $<10^{-3}$mm. Hg. If the hydrogen flow is to be directed through a refrigerated impurity trap, the material is now introduced into the trap and cooled to the desired temperature. The cold-finger window is oriented to face the spray, the manifold is opened to the flow line, and the hydrogen flow is begun. Oven heaters and microwave generators are energized at this time.

During film generation the deposition chamber is never isolated from its pumping station. Any degradation of the vacuum from desorbing hydrogen will increase heat conduction to the liquid helium bath, raising its temperature in turn increasing the rate of desorption until the liquid helium supply has boiled away, possibly at an explosive velocity.

At the completion of the deposition, ovens are turned off, discharges are quenched, and the flow is stopped by isolating the hydrogen line from the manifold. The

cold-finger is rotated 90° to line up with the optical path for spectral measurements. Upon illumination the hydrogen film is imaged on the spectrometer slit and absorption spectra are generated.

Once the liquid helium supply has boiled off and the hydrogen sublimed from the cold-finger, the complete system is evacuated and the cryostat is allowed to warm up to room temperature. Material in impurity traps is removed from the manifold if its presence at room temperature is troublesome. Also at room temperature the cryostat refrigerant cans are cleaned, as described above. The diffusion pumps, if they are to be shut down, are separated from the system and turned off. The cooling lines are usually kept operating.

4. ABSORPTION SPECTRA OF CALCIUM ISOLATED IN SOLID HYDROGEN

Of importance to an understanding of the chemical constituents of the interstellar medium is a reasonable explanation of the diffuse absorption features found in the extinction profile of stellar radiation due to the presence of interstellar dust particles. Two pieces of evidence indicate that the absorption features can be attributed to impurities within the dust material. They are: (1) a strong correlation between the strength of the absorption signals and the degree of interstellar extinction[1]; (2) a change in the magnitude of the interstellar polarization[1] at 4430A., the position of the most prominent diffuse absorption feature[2]. Reproduction of the fluctuations in the polarization profile of stellar radiation, mentioned above, by considering the effect of an impurity upon the polarization produced by an oriented, asymmetric dust particle has been achieved with partial success[3][4].

The chemical composition of the dust particles is still unknown. A possible constituent is solid hydrogen for the following reasons. In dark dust clouds there is much indirect evidence that a significant fraction of hydrogen exists in the molecular or solid form[5][6]. The question of the extent of solid hydrogen formation

on a dust particle is difficult to resolve since very little is known about the temperature of a dust particle in a dark cloud or even the amount of radiation loading it experiences.[6] However, from considerations of a resonant absorber lodged within a hydrogen matrix, fair agreement is obtained with the experimental extinction profile of the 4430A. band.[7]

As s study of the model of a resonant absorber at 4430A. in a hydrogen matrix, calcium atoms have been selected as the absorber since the free calcium atom exhibits a strong resonance transition ($4_s4_p\,^1P_1 \leftarrow 4_s^2\,^1S_o$) at 4227A. By generating a thin film of solid hydrogen with calcium impurities, the effect of the surrounding hydrogen matrix upon the shape and position of the calcium atom resonance transition is to be determined. A reproduction of the 4430 A. interstellar absorption band is sought.

EXPERIMENTAL

The procedure in obtaining absorption spectra of calcium atoms isolated in solid hydrogen is identical to that described in Section 3. An oven situated in the "spray" chamber (Section 2) functions as the source of calcium atoms. It consists of a coil of No. 6 tungsten wire enclosed in Pyrex by sandwiching the coil between two concentric sections of tubing and sealing the ends. Support is derived from Pyrex-encased wires extending from the ends of the coil through the chamber wall. One end of the oven is sealed and the other is oriented toward the cold-finger.

The clean oven is loaded with calcium metal in an inert helium atmosphere. The oxidized surface of calcium metal turnings is removed mechanically with a file and slivers small enough to fit into the 2-mm. bore of the oven are filed off.

The residue in the spent oven presumably consists of unevaporated calcium metal as well as simple calcium salts such as CaO, Ca_3N_2 and CaH_2. Since these ingredients will react with an aqueous solution of nitric acid to form soluble products, the oven cleansing operation is a rinsing with the above solvent. The drying procedure involves a distilled water washing, a methanol washing

and evacuation on the vacuum line at elevated temperatures.

A serious drawback exists with this particular oven design in that it is not possible to evaluate the calcium-atom effusion rate with much accuracy. The temperature of the oven is not uniform along the length of the coil, the center being much warmer since the electrical leads at the ends of the coil conduct heat to the atmosphere. Furthermore, no means to directly measure the oven temperature is provided.

A rough estimate of the proportion of the calcium mass flow to the hydrogen mass flow is made in the analysis presented in the Appendix. From its treatment of experiments in which the spectrum exhibits a single absorption line, it argues that the above proportion is consistent with calcium atoms well-isolated in a hydrogen matrix, a condition suggested by the single-line spectrum.

In the above-mentioned experiments, with an oven voltage in the range of 0.6 - 1.0 V. and a resulting current flow of 6-7 amps, as little as five minutes of deposition are required to produce an absorption signal. Generally 1-2 hours of deposition are used, however, to generate a strongly absorbing film. All these depositions have resulted from a hydrogen flow rate of 2.3 ml./min. STP which corresponds to a pressure of 3×10^{-5} mm. Hg in the deposition chamber.

Matrices exhibiting several absorption features have been generated during the first exploratory investigations of calcium imbedded in solid hydrogen. However, the electrical parameters for the oven are not as certain nor have these experimental results ever been duplicated under more controlled conditions. The voltage applied across the oven was in the range of 0.5 - 1.0 V.; the amperage was not recorded. The hydrogen flow rate was 13 ml./min. STP which produces a pressure of 2×10^{-4} mm. Hg in the deposition chamber, an increase of an order-of-magnitude over later chamber pressures. Very pronounced absorption spectra were produced in one half hour but considerable scattering of light was experienced in the illumination of films deposited in a period of one hour or more.

Visual observation of hydrogen-isolated calcium reveals a film brownish-orange in color which perhaps is influenced by light reflected from the copper heat shield. For dilute solutions in which one absorption signal is produced, the film is transparent. The earlier spectra which exhibit several lines correspond to heavily-fractured films from which considerable light scattering occurred.

The instrumentation employed in generating spectra consists of a 100 W. tungsten ribbon lamp to illuminate

the spectra, a Jarrell-Ash f/6.3 Czerny-Turner plane grating spectrograph to disperse the radiation, and Eastman Kodak Type 103a-F and Type 103a-O spectroscopic plates to detect the spectra. The 600 line/mm. grating is blazed at a wavelength of one micron, resulting in the illumination of the calcium spectrum in the second order of the dispersed radiation. The orders are separated with Corning glass optical filters with the linear dispersion in the second order of the spectral region of calcium-atom absorption being 0.049 mm./A., as determined from iron spectral line calibrations.

RESULTS

The principle interest in this investigation is the modification of the Ca I resonance line (λ_{air}= 4226.73A.) when calcium is imbedded in solid hydrogen. Five separate lines are perceived in this spectral region (Figure 4-2) presumably due to the presence of matrix-isolated calcium.

The feature farthest to the blue is the most intense, its position and shape illustrated in the microdensitometer tracing of Figure 4-1. The parameters to describe this asymmetrical line are listed and assigned appropriate values in Table 4-1. These values represent the center of an uncertainty with a relative magnitude of 0.25%, i.e., the 90% confidence limit in the above values is ±10 A. Inaccuracy in the measurement of the parameters stems from the signal noise in Figure 4-1 and from the omission of standardized spectra overlapping the calcium absorption feature.

The shape of the line is characterized by considerable asymmetry, the tail extending to higher energy. The sharp red edge marks a rise in $\sim$300 cm^{-1} from 10% to 100% maximum signal whereas the long blue tail spans $\sim$1000 cm^{-1} in falling back to 10% maximum.

Four much weaker lines are found to lower energy from

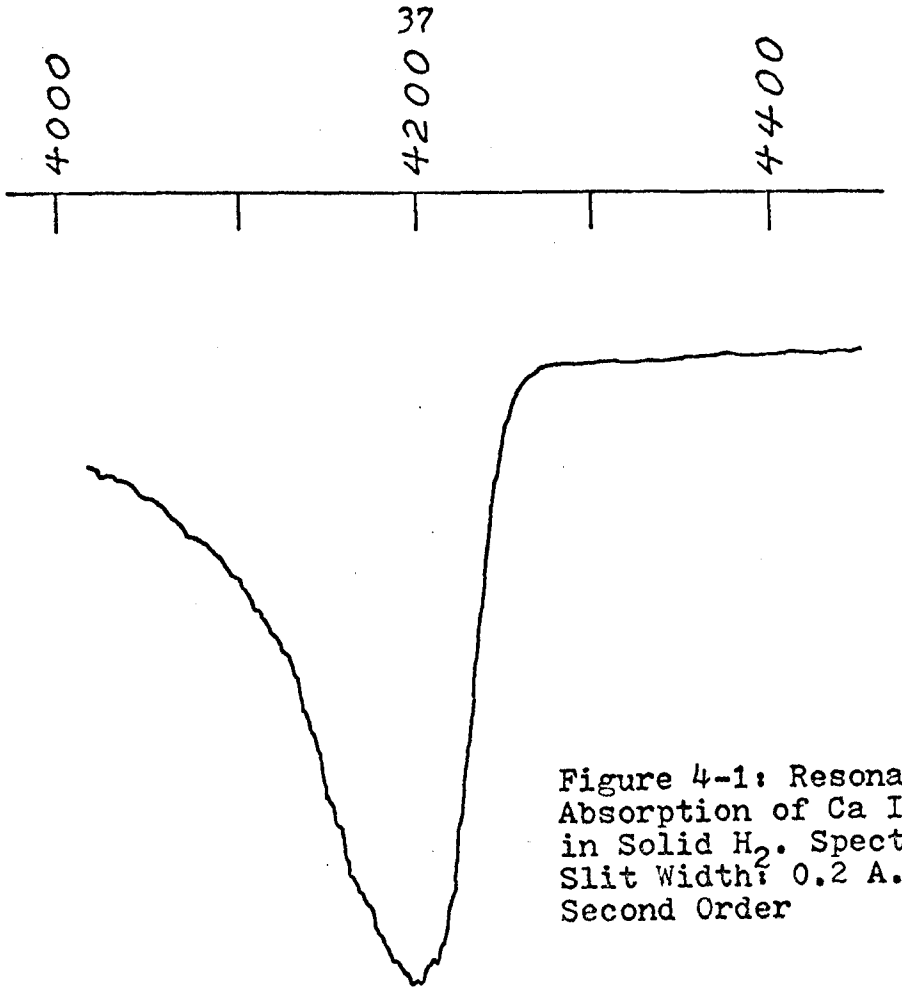

Figure 4-1: Resonance Absorption of Ca Isolated in Solid H_2. Spectral Slit Width: 0.2 A. in Second Order

	λ_{air}, A.	$\bar{\nu}_{vacuum}$, cm^{-1}
Peak Intensity	4203	23780
Line Width at Half Intensity	135	775
Center of Half Intensity Line Width	4174	23950
Line Width at 10% Maximum Intensity	230	1330

Table 4-1: Line Parameters for Ca Resonance Absorption in Solid H_2

the 4203 A. feature, the microdensitometer tracing of their absorption profiles being presented in Figure 4-2. The region of strong absorption between 3950 A. and 4300 A. is presumed to be the base of the principal 4203 A. signal. In Table 4-2 are listed the peaks of the four lines with an accuracy again limited by signal noise and absence of overlapping spectral standardization. It is estimated that a 90% uncertainty limit in these values would be $\pm$20 A.

Line No.	Wavelength, A.
1	4422
2	4448
3	4533
4	4785

Table 4-2: Absorption peak assignments for Ca isolated in solid H_2.

The widths of the four lines to lower energy are smaller than the 800 cm^{-1} width of the 4203 A. line by 50-75%. Only one of the lines, the lowest in energy, is isolated enough to permit measurement of its width, namely 90 A. Furthermore the center at 50% maximum intensity is at 4776 A., a value with a 0.2% uncertainty.

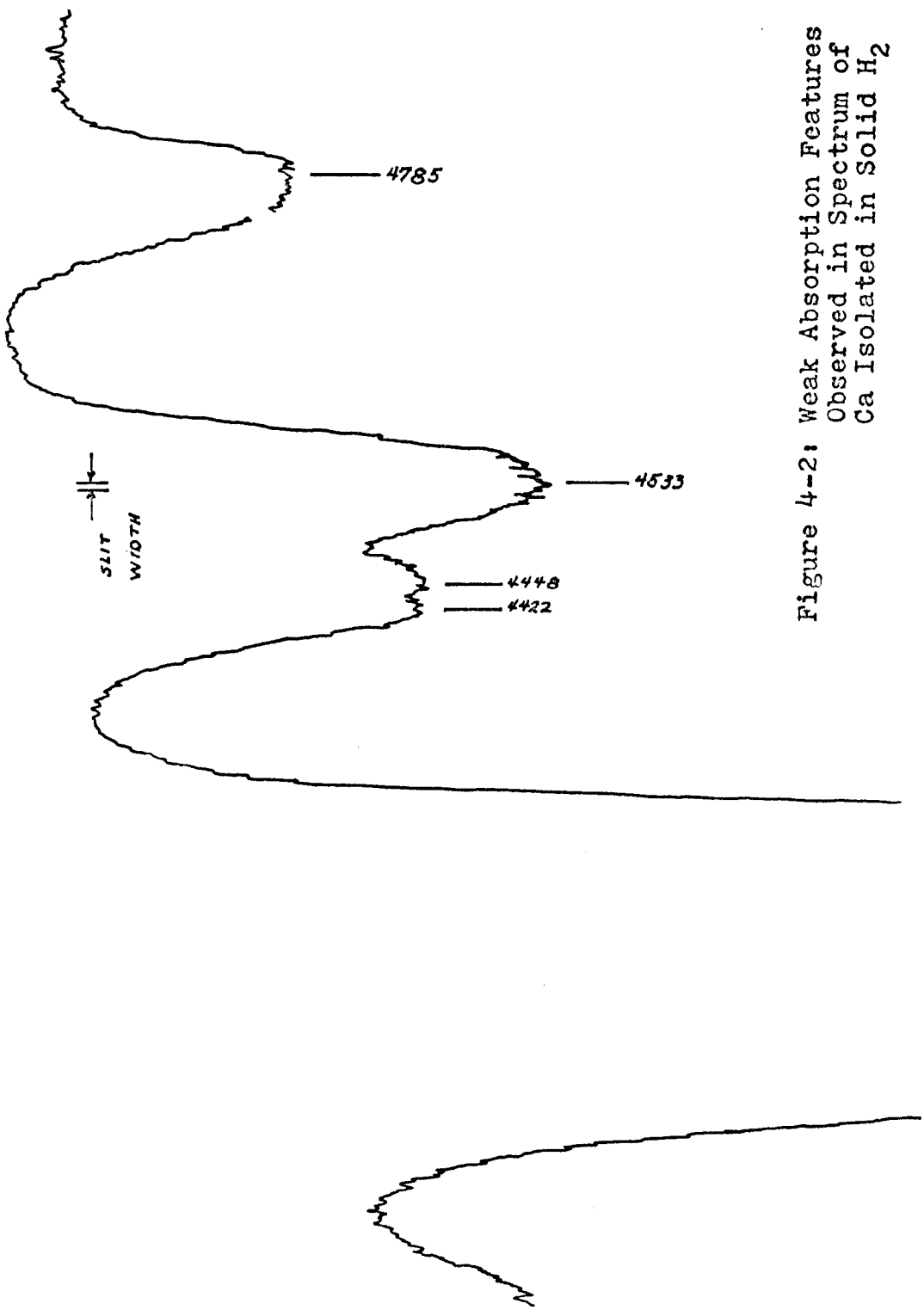

Figure 4-2: Weak Absorption Features Observed in Spectrum of Ca Isolated in Solid H_2

The other lines overlap to such an extent that the line shapes cannot be readily ascertained. A visual estimate of their half-widths would be as follows:

Line No.	Spectral Width, A.
1	40
2	50
3	100

Similarly the asymmetry found in the 4203 A. feature is likewise found in the weaker features to the red. The reddest line definitely reveals a degrading, or tail, to higher energy. The upper portion of the line peaking near 4530 A. gives an indication of a degradation to the blue. The possibility that this is due to overlap with the lines further to the blue cannot be dismissed, however.

RANDOM COMMENTS

The comparison between the absorption profile of calcium isolated in solid hydrogen depicted in Figure 4-1 and the profile of the diffuse interstellar absorption band at 4428 A. reproduced in Figure 4-3 reveals the unsuitability of the $Ca:H_2$ system as a source model of the diffuse feature. The discrepancy between the positions of the two peaks is 225 A., a value too large to be reasonably accounted for by differences in radial velocity between the diffuse absorber and the interstellar atoms used to calibrate the interstellar spectrum. As an illustration, the velocity shift between a star used to illuminate interstellar absorption spectra and its interstellar Na I lines amounts to 0.2 A.(11)

If the 4428 A. feature is actually the Ca I resonance transition perturbed by weak interactions between calcium

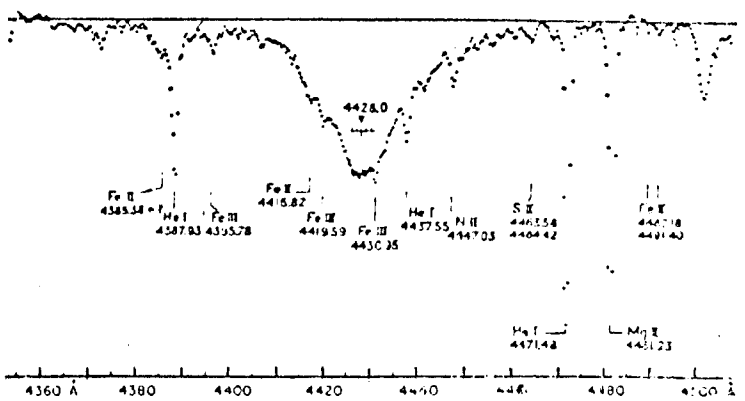

Figure 4-3: Profile of 4428 A. diffuse feature of interstellar absorption spectra(11)

and its environment, a medium of particles with a greater mean polarizability than that characterizing hydrogen would likely be required to red-shift the resonance transition[12] if dispersion forces are the sole attractive interaction. Or a reduction in the magnitude of the blue-shift resulting from repulsive exchange interactions would also suffice, i.e., situating a calcium atom into a more spacious site than available in solid hydrogen would likely result in a shift to lower energy. These conditions are not generally very restricting but they do argue against the applicability of calcium isolated in solid deuterium. Further discussion of systems isolated in hydrogen and deuterium may be found at the end of Section 5.

The absorption peak observed in the $Ca:H_2$ system is blue-shifted relative to the value for calcium in the unperturbed state. This is not unexpected, since the majority of spectral investigations of atoms isolated in low-temperature matrices result in a blue-shifted absorption signal.[13] These shifts to higher energy have been attributed to the large repulsive interactions an atom experiences when "squeezed" into a substitutional site in a close-packing lattice.[12] The difference between repulsions in the calcium ground and excited states presumably determines the direction in which the transition

is shifted. From considerations of atomic values in calcium metal[10], the atomic diameter of calcium in the ground state is estimated to be 3.94 A. which is larger than the intermolecular spacing of 3.75 A. in solid hydrogen, a condition that does not invalidate the above analysis.

The asymmetry characterizing the absorption profile in Figure 4-1 is indicative of an expansion in the size of the absorber upon excitation, judging from a recent theoretical investigation[14] which predicts a tailing to the blue for an absorbing impurity coupled to the surrounding lattice. Such an expansion would be expected in the excitation of a 4s electron to a 4p orbital in the calcium atom, the change in the electronic properties being passed on to the lattice through dispersion and exchange forces.

No account of any certainty can be presented for the four weaker lines to the red. Simple calcium compounds that may arise in deposition may be responsible. But it has been claimed that Ca_2 absorbs at 5000 A.[15] no other prominent absorption being reported. CaH_2, unstable under excitation in the free state, has never been studied in a matrix-isolation situation. But the ($\tilde{E}^2\Pi \longleftarrow \tilde{X}^2\Sigma$) transition in CaH occurs at 4900 A. in the gas phase, not far to the red of the feature at 4785 A. (Figure 4-2).

The isolation of an oversized molecule like CaH in solid hydrogen would be expected to show blue-shifted spectra. The 3900 A. transition of CaH is not seen but may be obscured by the strong calcium absorption at 4203 A. or by the spectral filters used.

The most likely explanation for the existence of these lines is the occurrence of multiple sites in the hydrogen matrix. As noted in the description of experimental conditions, the film that exhibited these weak signals was frosted in appearance, suggesting the existence of many lattice defects in which calcium may reside. In generating these films, the calcium oven was initially overheated in the search for the proper voltage. Not only would this supply an overabundance of calcium atoms to the film resulting in a heightened frequency of lattice distortions but a unoxidized surface of calcium metal would be provided resulting in a lessened barrier to calcium evaporation during subsequent deposition at the reduced voltage. For a given deposition period, stronger absorption features would then be expected. It is essential in the elucidation of the nature of these weak lines that the depositions be repeated under more well-defined heating conditions.

APPENDIX

During oven operation the central third of the coil is luminescent. As a working model it is assumed that the glowing part of the coil is the source of oven heat, while the temperature of the remainder does not rise. Such an assumption offers an upper limit to the temperature of the central coil fraction.

In experiments in which well-isolated calcium atoms are evidenced by a single absorption feature, the voltage across the coil is one volt, the current is six amps, and the resistance to current flow has increased by a factor of 0.17 over the resistance offered at room temperature. The resistivity rise of the heated fraction of the coil model that duplicates the measured rise in coil resistance is a factor of 3.0. Since tungsten resistivity is a monotonically increasing function of temperature, this three-fold increase indicates the limit to oven operating temperature is 700°K. with a 25°K. confidence limit in the interpolation of resistivity data at various temperatures.[8]

Further assumptions are necessary in the consideration of the mode of calcium effusion from the oven. Because it is observed that calcium metal coats the entire length of the oven bore once it is fully heated, it is supposed that the calcium effusion rate is moderated by the

temperature of the glowing-red fraction. Then the determination of the rate of effusion, if it is equated to the rate of evaporation of calcium atoms from the warmest metal surface, should yield a maximal value since no consideration of calcium condensation within the oven is being made. Calcium evaporation from cooler parts of the oven is ignored which would otherwise partially compensate for the omission of the effect of condensation, but it is probably a small contribution since the evaporation rate drops rapidly with temperature, i.e., an order-of-magnitude decrease with a 50°K. drop in temperature.

If the heated fraction of the oven is characterized by a temperature of 725°K., then the vapor pressure[9] and the evaporation rate[10] of calcium atoms from the heated metal surfaces are 0.11 microns Hg and 1.4×10^{-8} mole-sec^{-1}, respectively. The latter value is the estimated upper limit to the rate of calcium effusion from the oven.

The comparison of this value with the hydrogen flow rate characterizing the above experiment, 1.7×10^{-6} mole-sec^{-1}, suggest that the two substances strike the cold-finger in a ratio of 100:1, a value to be taken as minimal. Further consideration reveals that this ratio does not necessarily describe the final proportion in the hydrogen matrix. For example, the particle "sprays" are

not similar in that the calcium "spray" is more compact like a particle beam. In conjunction with the fact that the calcium source is closer to the cold-finger than is the hydrogen source, this indicates that the calcium flux is greater at the cold-finger than is suggested by the above comparison of flow rates. This has the effect of lowering the above ratio. Also the adhering efficiencies differ between calcium and hydrogen particles. If the difference is large, this will also reduce the ratio.

An accurate estimate of the final impurity fraction is not possible with the available experimental data. The above analysis, however, does suggest that the calcium flow is small enough to allow successful isolation of individual calcium atoms in the hydrogen film.

REFERENCES

1. N. H. Dieter, W. M. Goss, Rev. Mod. Phys. 38, 256 (1966).
2. K. Nandy, H. Seddon, Nature 227, 264 (1970).
3. N. C. Wickramasinghe, K. Nandy, Nature Physical Science 229, 234 (1971).
4. A. Kelly, Astrophysics and Space Science 13, 211 (1971).
5. G. R. Carruthers, Space Science Reviews 10, 459 (1970).
6. P. M. Solomon, N. C. Wickramasinghe, Astrophys. J. 158, 449 (1969).
7. N. C. Wickramasinghe, K. Nandy, Astrophys. and Space Sci. 6, 154 (1970).
8. C. D. Hodgman, Ed., Handbook of Chemistry and Physics, Chemical Rubber Publishing, 1960.
9. An. N. Nesmeyanov, Vapor Pressure of the Elements, Academic Press, 1963.
10. S. Dushman, Scientific Foundations of Vacuum Technique, Wiley and Sons, 1962.
11. G. H. Herbig, Zeit. fur Astrophys. 64, 512 (1966).
12. G. W. Robinson, J. Molec. Spectrosc. 6, 58 (1961).
13. B. Meyer, Low Temperature Spectroscopy, American Elsevier, 1971.
14. J. M. Schurr, Int. J. Quantum Chem. 5, 221 (1971).
15. W. J. Balfour, R. F. Whitlock, Chem. Comm., p. 1231 (1971).

5. ABSORPTION SPECTRA OF BENZENE ISOLATED IN SOLID HYDROGEN

The intriguing aspect of the absorption spectrum of matrix-isolated benzene in the 2500 A. region is the extremely fine structure characterizing each vibronic transition. The widths of the individual lines are among the narrowest exhibited in matrix-isolation spectra, widths less than a wavenumber in magnitude having been obtained.[1] And the line spacings within the fine structure lie between 10 and 100 cm^{-1}, a relatively small (0.03%-0.3%) fraction of the transition energy.

Predominant in these spectra of the transition from the totally-symmetric ground state, $\widetilde{X}\,^1A_{1g}$, to the first excited singlet state, $\widetilde{A}\,^1B_{2u}$, is a progression of the ν_2 totally symmetric vibration of 923 cm^{-1} amplitude superimposed upon one quantum of an e_{2g} (point group D_{6h}) vibration of $\sim$516 cm^{-1} in the excited electronic state. A record of the spectral measurements of the e_{2g} vibronic origin for matrix-isolated benzene is presented in Table 5-1.

Multiplet structure in the vibronic components of the $\widetilde{A}\leftarrow\widetilde{X}$ transition has been observed in all the solvent mediums listed in Table 5-1. A separation of roughly 100 cm^{-1} between two prominent features in the structure is shown by all benzene mixtures. Investigators have speculated

Table 5-1: Properties of the e_{2g} Vibronic Origin for the $\tilde{A}^1B_{2u} \leftarrow \tilde{X}^1B_{2u}$ Transition of C_6H_6 Isolated in Various Solvents

Solvent Medium	Line Position[a]	Deposition Temperature	Multiplet Spacings	Intensity[b]	Line Width[c]	Reference
gas	38611 cm^{-1}					1
crystal	38331	4.2°K.				2
Ar	38478	"	(triplet) 0 cm^{-1}	25	s	3,4
				1	b	
			100	10	s	
	38500	20	0	s	s	5[d]
			40	w	b	
			82	s	s	
		4.2	0	s		"
			40	w		
			82	m		
	38502	"	0	s	s	6
			82	m	s	
	38498	20	0	s	s	7[e]
			86	s	s	
	38495	25	0	s	b	"
			86	s	s	
	38495	30	0	s	b	"
			87	s	s	
Kr	38360	4.2	(triplet)			4
Xe	38215	"				"
CH_4	38311					"

N_2	38471	20.4	(singlet)		s	8
	38469	17.5	0	s	s	"
			94	s	s	
	38470	4.2	0	s	s	"
			95	m	s	
H_2	38499	2	0	m		3
			68	s	s	
			77	s	s	
			89	s	s	
			99	s	s	

a. Reddest multiplet component
b. s=strong; m=moderate; w=weak
c. s=sharp; b=broad
d. Other solvent mediums investigated are Kr, Xe, CO_2, CH_4, and N_2.
e. Temperature effects in Kr environment are discussed.

1. F.M.Garforth et al, J.Chem.Soc., p.406, (1948)
2. H.Sponer, Rev. Mod. Phys. 13, 75 (1941)
3. R.P.Frosch, Ph.D. Thesis, California Institute of Technology, 1965
4. G.W.Robinson, J. Molec. Spectrosc. 6, 58 (1961)
5. O.Schnepp, J. Molec. Spectrosc. 18, 158 (1965)
6. C.E.Blount, J. Molec. Spectrosc. 19, 456 (1966)
7. " , J. Molec. Spectrosc. 35, 61 (1970)
8. " , J. Molec. Spectrosc. 25, 269 (1968)

upon the nature of this structure. The dependences upon the deposition temperature as well as subsequent film temperatures, upon the solute concentration, and upon the degree of matrix annealing have been studied. Correlations between measurements in different solvents and solvent mixtures and between absorption and emission studies have been sought. Yet little agreement has been achieved. The origin of multiplet structure is still not understood.

Further work in the investigation of hydrogen-isolated benzene absorption is the substance of the present report. Only a cursory examination of this system has been performed, as referenced in Table 5-1. Not only is the multiplet structure richer in detail in this medium but hydrogen offers the opportunity to study the effects of solvent isotopic substitution and even the effect of hydrogen molecules in different rotational states, i.e. ortho- and para-hydrogen, neighboring the benzene absorber. Such studies bear upon the nature of the multiplet structure and, in turn, upon speculations concerning the structure observed in other light matrices.

EXPERIMENTAL

The procedure for the generation of samples of benzene isolated in solid hydrogen is described in Section 3, the apparatus in Section 2. Benzene is introduced into the vacuum manifold at the site of a trap (see Section 2) which has been installed along the line of hydrogen flow. The actual introduction is effected with the illustrated vacuum glassware. The sample tube B is sealed to the

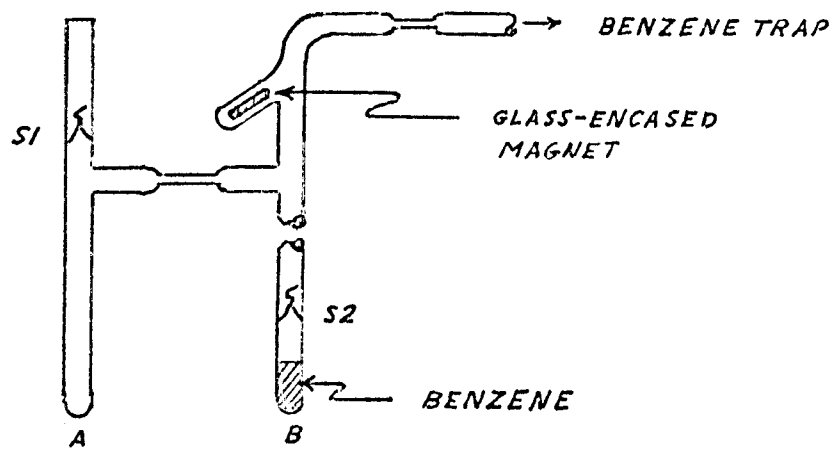

manifold vacuum system at the indicated position and the manifold is pumped out. Previously, the benzene sample has been purified on a separate vacuum system and vacuum distilled into sample tube B. When a benzene-hydrogen deposition is to be performed, the break-seal S2 is opened with the externally-controlled magnet and benzene is vacuum distilled into the benzene trap. When benzene is

to be removed from the manifold, it is vacuum distilled into the sample tube A which is then separated from the manifold at the constriction between tubes A and B. The sample is now isolated from the atmosphere behind break-seal S1 and can be attached to the manifold as sample tube B at some future need.

When there are periods of several days between experiments, it is important that the benzene vapor pressure in the manifold is maintained at a low value. The large solubility of benzene in vacuum grease, in particular the Apiezon greases, can degrade the manifold vacuum since a fluid mixture of benzene and grease can result with a loss of sealant about the ground-glass vacuum joints. Consequently, either the benzene trap should be constantly refrigerated during periods of inactivity or it can be removed from the manifold in the above manner.

In the majority of experiments in this study, the benzene trap is refrigerated with an isopropanol-dry ice mixture. The vapor pressure of benzene at this temperature (-78.5°C.) is 0.005 mm. Hg.[2] Since the manifold pressure under hydrogen flow conditions levels off at ~6 mm. Hg, the hydrogen-benzene flow ratio is approximately 1000:1. In the instances in which deuterium is substituted as the solvent medium, the steady-state flow conditions yield a

pressure of ~2 mm. Hg in the manifold, resulting likewise in a small value for the mole fraction of benzene in solution.

Investigations into the fine structure exhibited by perdeuterobenzene in solid hydrogen or deuterium have also been carried out. The solute is introduced into the manifold in the manner described above. And refrigeration is likewise effected with a dry ice bath under the assumption that perdeuterobenzene possesses a vapor pressure comparable to that of benzene at this temperature.

The system modifications involved in initial studies of the effect of the ortho- and para-hydrogen proportions in the solid solvent on the benzene spectrum only concern the hydrogen gas line preceding the capillary leak L1 (see Figure 2-2). The scheme is to reduce through heterogeneous catalysis the room temperature ortho/para ratio of hydrogen gas of 3:1 to the 1:1 ratio exhibited by hydrogen in complete thermal nuclear-spin equilibrium at the boiling point of liquid nitrogen. A highly efficient ortho-to-para conversion catalyst[3], consisting of nickel oxide-silica particles, was obtained from the chemical group of Air Products and Chemicals, Inc. The pyrex chamber, 8 cm. in length, containing the catalyst bed is installed in the hydrogen gas line in the illustrated manner to allow its immersion into a liquid nitrogen bath. To enable the hydrogen gas

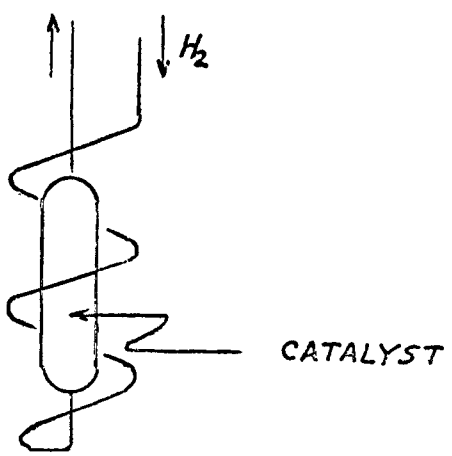

temperature to drop before the gas percolates through the catalyst bed, the flow line immediately preceding the chamber is fashioned as a heat transfer coil. The chamber is removable from the gas line with the use of swagelock fittings with teflon ferrules to enable the introduction or removal of catalyst.

At a hydrogen flow rate of 2.3 ml./min. STP and a line pressure of one atmosphere, hydrogen gas is in contact with the catalytic material sufficiently long to provide a hydrogen flow characterized by an ortho/para ratio of 1:1. This conclusion results from extrapolations of literature conversion efficiencies[3], as no direct measurements were made. The chamber is oriented vertically to minimize the channeling of gas through the bed which would otherwise degrade the conversion. Another precaution is the mounting of a liquid nitrogen trap between the catalyst and the hydrogen capillary flow leak to insure that no

benzene by backstreaming from the manifold will poison the catalyst.

Since air components such as nitrogen and water can poison the catalyst as well, an activation procedure is required. To remove moisture, the catalyst is purged with dry nitrogen at an elevated temperature (150-200°C) for a period of a few hours. The subsequent removal of nitrogen is effected by purging with hydrogen but at room temperature since the contact of catalyst with hydrogen at elevated temperatures will result in significant chemical reduction. And finally before initiating a hydrogen deposition, the hydrogen feed line and catalyst chamber are well evacuated.

In all the investigations in this report, the hydrogen or deuterium flow is sufficiently low to maintain a vacuum condition in the deposition chamber, namely $\sim 5 \times 10^{-5}$ mm. Hg. Furthermore since the mixing ratio of benzene in hydrogen is small, a deposition period of 4-5 hours is required to produce a strong absorption signal in the 2500A. region.

To obtain the absorption spectrum, the film is illuminated with the ultraviolet continuum from a hydrogen discharge lamp. The radiation traversing the sample is focussed onto the entrance slit of a diffraction grating spectrograph with a Czerny-Turner optical mounting and a focal length of two meters. The grating possesses a line spacing of 600/mm. and is blazed for one micron radiation.

The 2500A. transition of benzene is measured in the third order of diffracted light with a third order linear dispersion of 0.391-0.395 mm./Angstrom. The orders are filtered with a combination of a chlorine gas filter and a transmission filter consisting of $NiSO_4$ and $CoSO_4$ in aqueous solution.[4] And the spectra are recorded photographically with Eastman Kodak Type 103a-0 spectroscopic plates.

Hydrogen and deuterium flows are obtained from high-purity cylinders without further purification.* The hydrogen, purchased from the Linde gas division, is derived from the boil-off of liquid hydrogen and is better than 99.95% pure. Deuterium gas, CP grade, is supplied by Matheson Gas Products who stipulate an atom purity of 99.5%. Purification procedures with benzene and perdeuterobenzene entail a reflux over fluid cesium followed by vacuum distillation before their introduction into the vacuum manifold in the manner described above.

*In the experiments investigating the effect of the ortho/para ratio reduction, the hydrogen flow does pass through two liquid nitrogen traps before entering the manifold.

RESULTS

The 2500A. absorption band of benzene isolated in solid hydrogen exhibits features similar to those reported in the studies referenced in Table 5-1. The strongest features expected in this band, namely a progression of the totally symmetric breathing vibrational mode superimposed upon a vibronic transition involving the simultaneous excitation of the $^1B_{2u}$ electronic state and one quantum of an e_{2g} vibrational mode reportedly 516 cm^{-1} in magnitude in the excited electronic state, are the only features observed in the present investigation. With regard to the first three transitions of this series, the similarities include the relative intensity relationships or Franck-Condon envelope, the vibrational spacings in the progression, and the presence of doublet structure of $\sim$100 cm^{-1} separation in each transition under low resolution. With greater resolution, each doublet component reveals additional fine structure. To lower energy the component splits into a doublet, the member to the red being the much weaker of the two; to higher energy the component consists of five well-resolved and uniformly spaced lines of $\sim$10 cm^{-1} separation. The positions of these lines, as recorded in Table 5-2, are in close agreement with the lines measured by Mr. Frosch

Table 5-2: Line Positions for the $\tilde{A}^1B_{2u} \leftarrow \tilde{X}^1A_{1g}$ Transition of C_6H_6 Isolated in Solid H_2.

No.	Vibronic Assignment	λ_{air}, A.	$\bar{\nu}_{vacuum}$, cm^{-1}
1	$0,0+e_{2g}$	2590.08	38597.3±0.3
2		2590.73	38587.6±0.6
3		2591.41	38577.5±0.6
4		2592.10	38567.2±0.7
5		2592.74	38557.7±0.7
6		2596.90	38495.9±0.7
7		a	a
1	$0,0+e_{2g}+a_{1g}$	2529.57	39520.5±0.9
2		2530.21	39510.5±0.3
3		2530.85	39500.5±0.6
4		2531.56	39489.5±0.9
5		2532.14	39480.4±0.9
6		2536.1	39419
7		a	a
1	$0,0+e_{2g}+2a_{1g}$	2471.73	40445.3±0.7
2		2472.4	40435
3		2473.0	40424
4		2473.7	40413
5		2474.2	40405
6		2478.0	40343.1
7		a	a

a. The line appears as a weak shoulder.

(Table 5-1). The differences in the relative intensities among the five blue multiplet lines, however, are more pronounced. Comparison can be made by observing the tracing on pg. 87 of Mr. Frosch's thesis[5] with the tracing provided in Figure 5-1a. The absorption profiles of the fine structure for the three vibronic transitions are very much alike.

In the investigation of benzene in solid deuterium, the observed absorption signals are roughly the same as in solid hydrogen. Vibronic line separations are identical and each transition in gross detail consists of a doublet ($\Delta\bar{\nu} \sim 100$ cm^{-1}). But as evidenced in Figure 5-1, the doublet spacing is greater, the red component moving to lower energy and the blue to higher energy. Under higher resolution the doublet breaks up into the familiar 2:5 line arrangement. The five lines to the blue are much weaker relative to the continuum, however, the line to highest energy appearing as a shoulder. In contrast, the fine doublet to the red is much more prominent and the component to lower energy is now the stronger of the two. The line positions are recorded in Table 5-3, indicating that the spacings in the five-line grouping are again roughly 10 cm^{-1}.

Comparison with vibronic transitions to higher energy in the solid deuterium medium reveals the decreasing

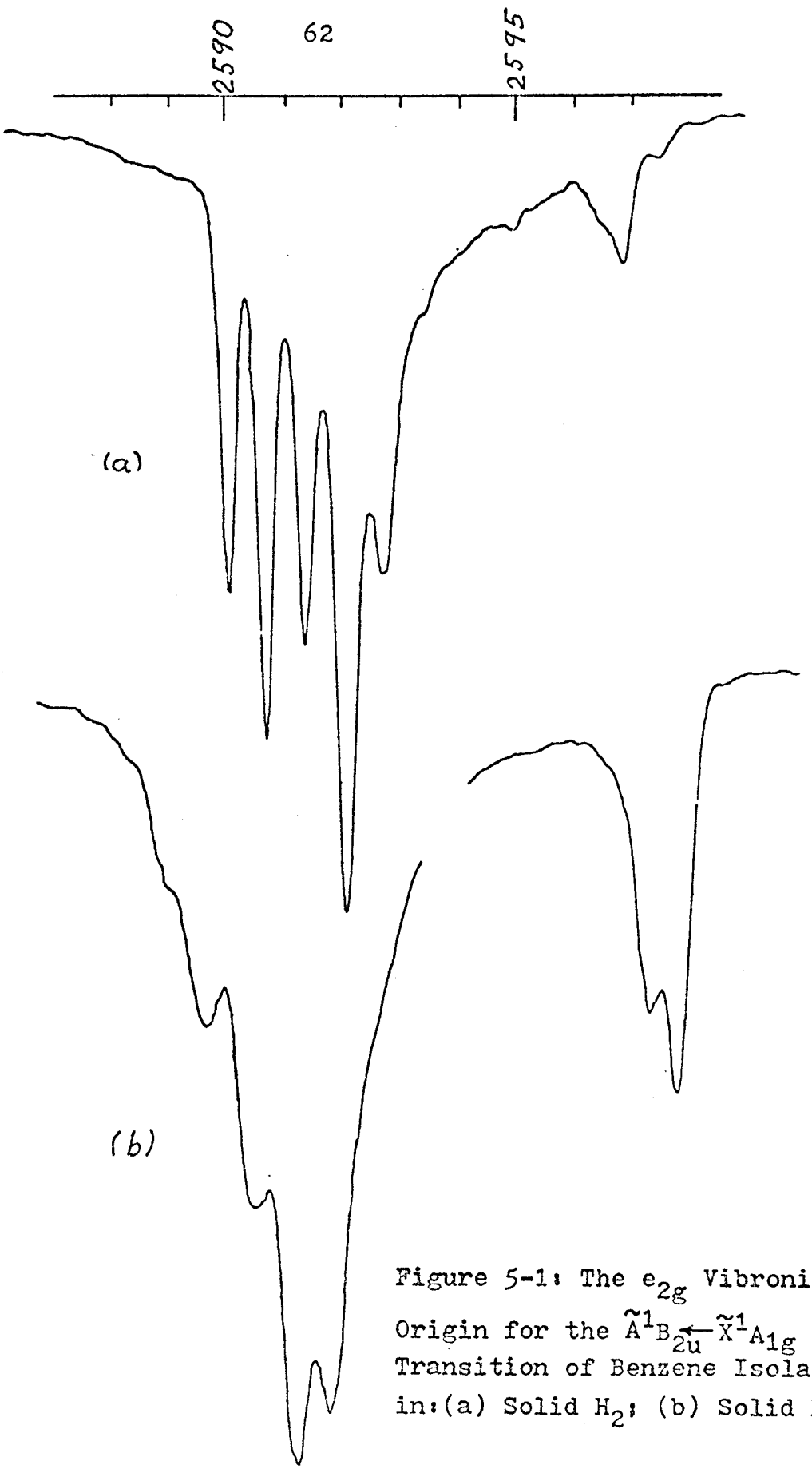

Figure 5-1: The e_{2g} Vibronic Origin for the $\tilde{A}^1B_{2u} \leftarrow \tilde{X}^1A_{1g}$ Transition of Benzene Isolated in: (a) Solid H_2; (b) Solid D_2.

Table 5-3: Line Positions[a] for the $\hat{A}^1B_{2u} \leftarrow \hat{X}^1A_{1g}$ Transition of C_6H_6 Isolated in Solid D_2.

No.	Vibronic Assignment	λ_{air}, A.	$\bar{\nu}_{vacuum}$, cm^{-1}
1	$0,0+e_{2g}$	b	b
2		2589.7	38604
3		2590.5	38591
4		2591.24	38580.0±0.4
5		2591.8	38572
6		2597.4	38489
7		2597.9	38482
1	$0,0+e_{2g}+a_{1g}$	b	b
2		2529.3	39525
3		2530.0	39514
4		2530.7	39503
5		2531.2	39494
6		2536.49	39412.7±0.3
7		2536.9	39406
1	$0,0+e_{2g}+2a_{1g}$	2470.7	40462
		2470.9	40458
2		2471.6	40447
3		2472.4	40435
4		2472.9	40426
5		2473.3	40419
6		2478.3	40338
7		2478.84	40329.3±0.04

a. The line numbering scheme is identical to that presented in Table 5-2 to reflect the similarity in fine structure patterns. Additional lines are included without number assignments.

b. The line appears as a weak shoulder

strength of the fine structure relative to the continuum. Excitation of two quanta of the a_{1g} mode yields a spectrum marked by a strong continuum to the blue, the fine structural lines, now six in number, reduced to shoulder-like features. Furthermore, the red doublet is no longer well-resolved but the members display the same relative strengths.

The spectral results for the isolation of perdeuterobenzene in solid hydrogen and deuterium are illustrated in Figure 5-2. From the line positions provided in Table 5-4 and 5-5, the vibrational spacings in the totally-symmetric mode progression do not differ greatly from the gas-phase value of 879 cm^{-1}.[6] With solid hydrogen as the solvent, the structure in the vibronic origin of perdeuterobenzene, other than being shifted by 179 cm^{-1} to the blue, is very similar to that exhibited in the benzene-solid hydrogen system (Figure 5-2a). The fine structure lines are well-resolved, they exhibit the same relative strengths, and a weak shoulder marks the member to lower energy of the red doublet. With the simultaneous excitation of one quanta of the a_{1g} motion, a spectrum differing from that of benzene is obtained (Figure 5-3). Now the strong signal to higher energy is characterized by eight well-resolved lines, still showing the same 10 cm^{-1} separation (Table 5-4). The five lines at the peak of the

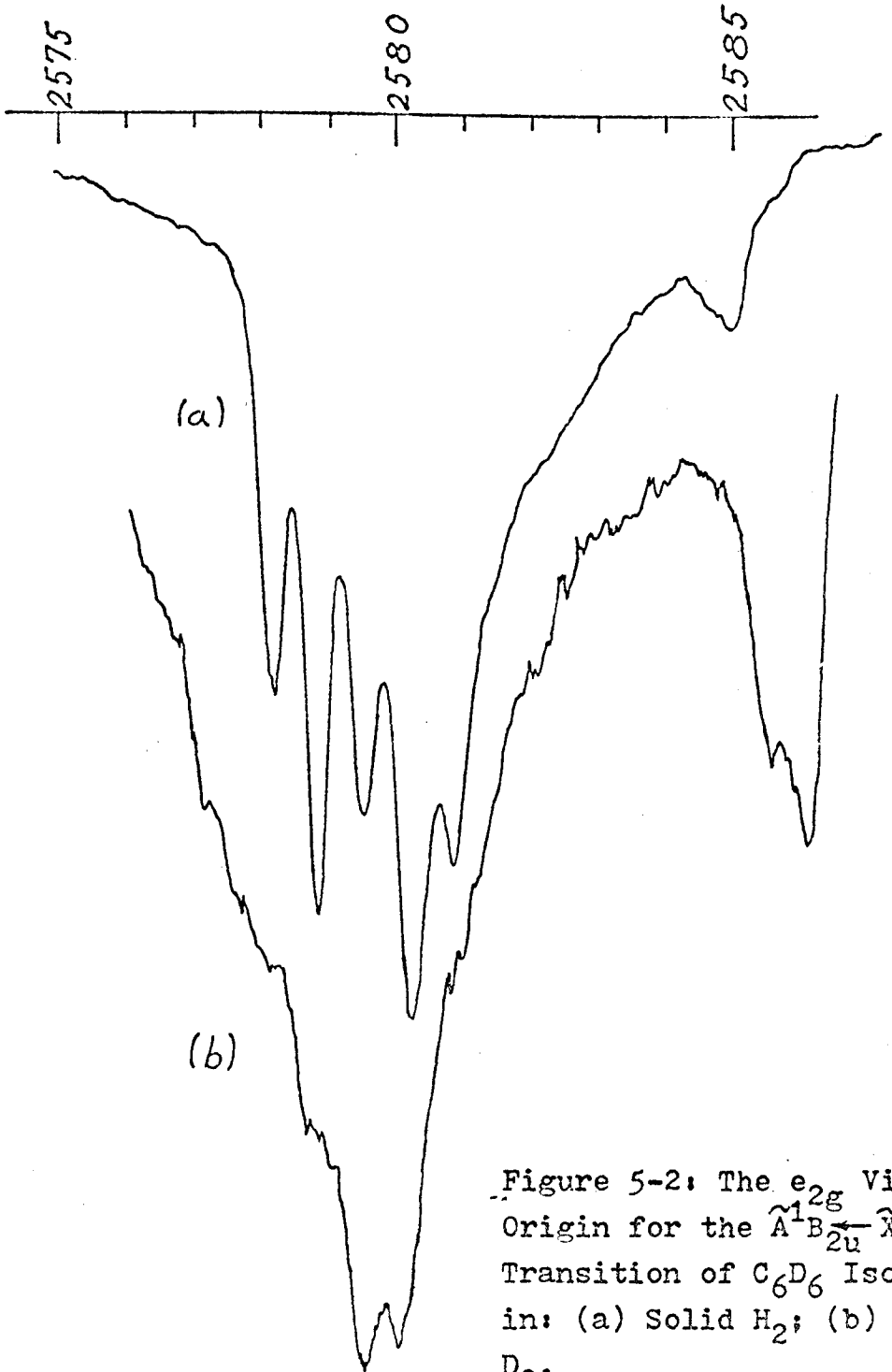

Figure 5-2: The e_{2g} Vibronic Origin for the $\tilde{A}^1B_{2u} \leftarrow \tilde{X}^1A_{1g}$ Transition of C_6D_6 Isolated in: (a) Solid H_2; (b) Solid D_2.

Table 5-4: Line Positions[a] for the $\tilde{A}\ ^1B_{2u} \leftarrow \tilde{X}^1A_{1g}$ Transition of C_6D_6 in Solid H_2

No.	Vibronic Assignments	λ_{air}, A.	$\bar{\nu}_{vacuum}$, cm^{-1}
1	$0,0+e_{2g}$	2578.09	38776.2 ± 0.3
2		2578.76	38766.7 ± 0.6
3		2579.45	38756.4 ± 0.6
4		2580.18	38745.4 ± 0.6
5		2580.8	38737
6		2584.9	38675
7		b	b
	$0,0+e_{2g}+a_{1g}$	2518.2	39700
		2519.0	39687
		2519.7	39675
1		2520.89	39656.6 ± 0.8
2		2521.52	39646.7 ± 0.3
3		2522.26	39635.1 ± 0.8
4		2522.9	39625
5		2523.5	39616
6		2527.3	39556
7		b	b
c	$0,0+e_{2g}+2a_{1g}$	2463.8	40575
		2464.8	40560
		2465.4	40550
		2466.3	49534
		2466.9	40525
		2467.4	40516
		2468.16	40503.8 ± 0.4
		2472.2	40438

a. The line numbering scheme is identical to that presented in Table 5-2 to reflect the similarity in fine structure patterns. Additional lines are included without number assignments.

b. The line appears as a weak shoulder.

c. The pattern of fine structure bears little resemblance to structure observed in the other vibronic transitions.

Table 5-5: Line Positions[a] for the $\tilde{A}\,^1B_{2u} \leftarrow \tilde{X}\,^1A_{1g}$ Transition of C_6D_6 Isolated in Solid D_2.

No.	Vibronic Assignments	λ_{air}, A.	$\bar{\nu}_{vacuum}$, cm^{-1}
1	$0,0+e_{2g}$	b	b
2		b	b
3		b	b
4		2579.4	38756
5		2579.95	38748.8±0.6
6		2585.5	38666
7		2586.1	38657
1	$0,0+e_{2g}+a_{1g}$	b	b
		2520.2	39667
2		2520.6	39661
3		2521.4	39649
4		2522.2	39635
5		2522.6	39629
		2523.0	39623
6		2527.9	39546
7		2528.34	39539.8±0.7
	$0,0+e_{2g}+2a_{1g}$	c	c

a. The line numbering scheme is identical to that presented in Table 5-2 to reflect the similarity in fine structure patterns. Additional lines are included without number assignments.

b. The line appears as a weak shoulder

c. A continuum extending from 40500 cm^{-1} to 40600 cm^{-1}

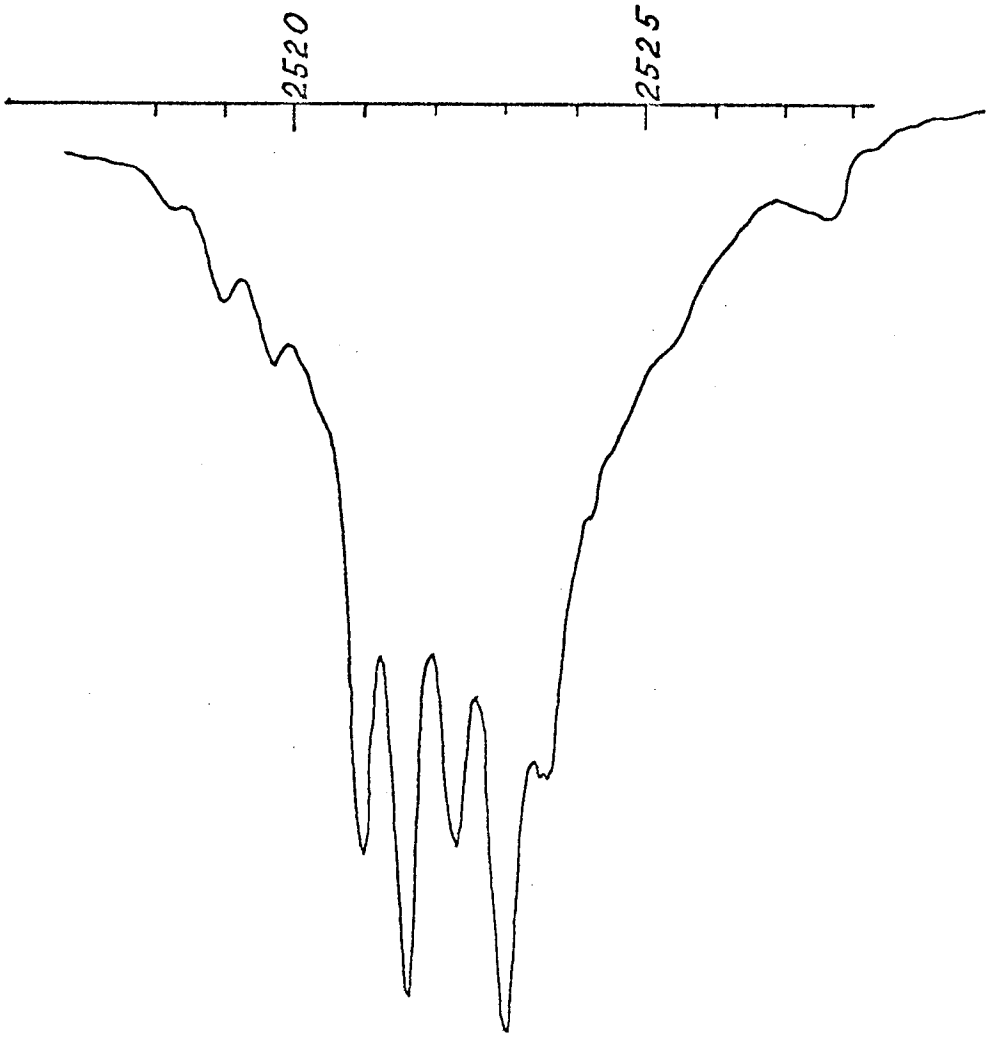

Figure 5-3: The (0,0 + e_{2g} + a_{1g}) Vibronic Component of the $\tilde{A}^1B_{2u} \leftarrow \tilde{X}^1A_{1g}$ Transition of C_6D_6 Isolated in Solid H_2.

background continuum appear to correspond to the five lines seen in the vibronic origin as they are about the same distance from the prominent red line and exhibit the same relative line strengths. The same arrangement can be observed in the excitation of two quanta of the a_{1g} vibration despite the expected decrease in line strength.

The above trends are duplicated in the system of perdeuterobenzene isolated in solid deuterium. In comparison to perdeuterobenzene in solid hydrogen, the overall doublet structure ($\Delta\bar{\nu} \sim 100$ cm^{-1}) shows a larger separation, the red again moving to lower energy, the blue to higher. The lines to the blue are weak relative to the underlying continuum, the presence of three out of the five lines evidenced by shoulders (Figure 5-2b). Because the background is strong, the anomalous blue fine structure mentioned above for perdeuterobenzene in solid hydrogen is difficult to discern, but six structural features are resolved and more are suggested by shoulders. As expected from the work with benzene, the red doublet is strong in the deuterium system and the components are resolved (Figure 5-2b), the red member the most intense.

In the above four systems some of the line positions have been tabulated in conjunction with uncertainty values. All spectral plate measurements were made with

confidence limits of 90%. The limits recorded in Tables 5-2 through 5-5 result from standard propagation-of-error considerations in the arithmetic involved in evaluating spectral positions. Those table entries that are accorded uncertainty values indicate strong symmetrical lines whose centers can be determined. A position without an error limit indicates a weak line whose peak intensity is measured with an accuracy of roughly 1-2 cm^{-1}. Transitions greater in energy than those listed are omitted because spectral standards in this region were not used.

The results of the investigation into the effect of reducing the ortho/para ratio of the solid hydrogen environment are illustrated in Figure 5-4. With benzene in a medium consisting of a 1:1 mixture of ortho- and para-hydrogen, the familiar fine structure pattern is again seen, the lines occurring at the same positions and with the same sharpness as with benzene embedded in a hydrogen medium characterized by a room temperature ortho/para ratio. But the line strengths are dramatically altered. Line 1 in Figure 5-4 is greatly reduced in intensity while lines 3 and 5 appear to gain intensity relative to lines 2 and 4. In addition, the more intense component of the red doublet decreases in strength. The above description is applicable to all the vibronic transitions of benzene presently considered.

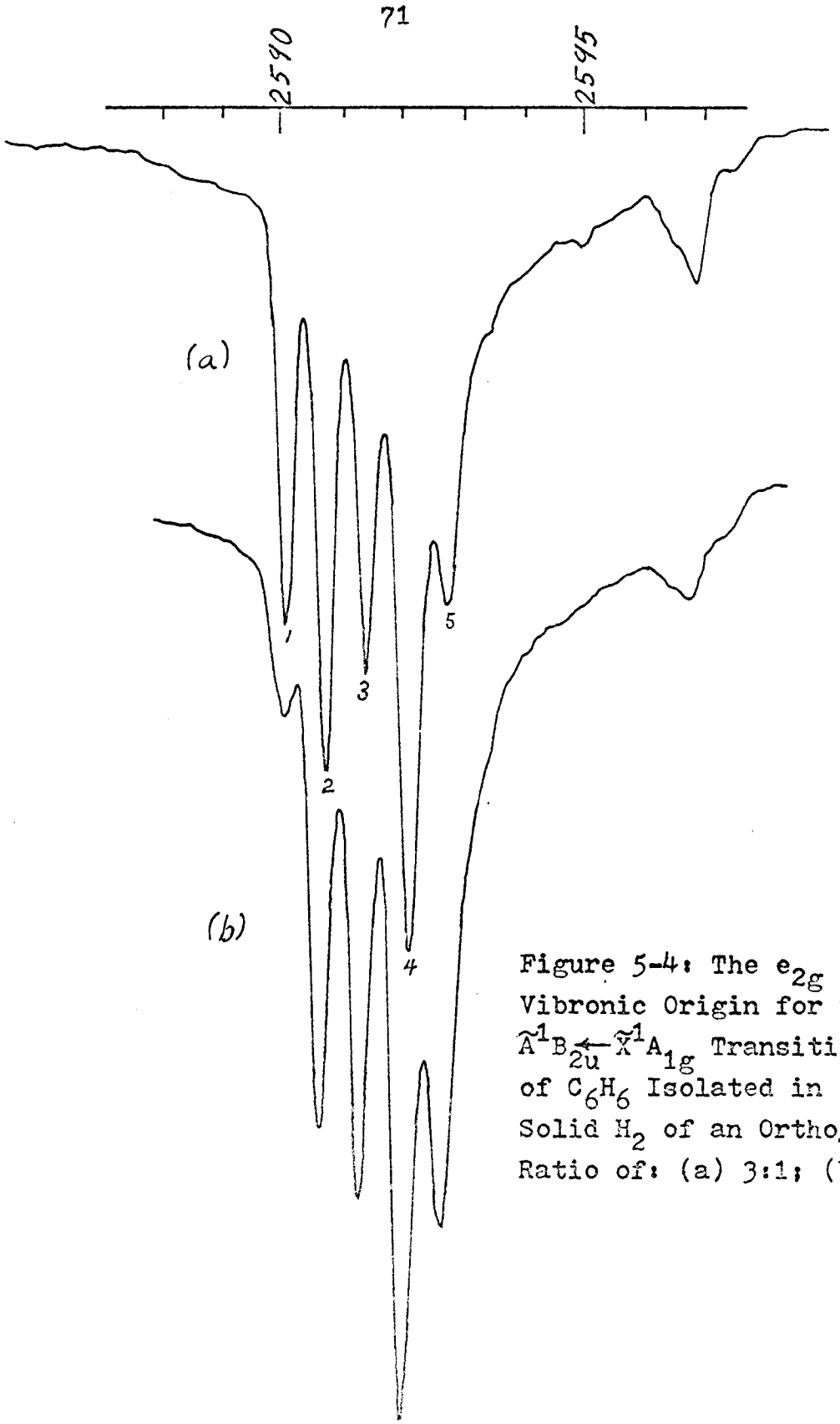

Figure 5-4: The e_{2g} Vibronic Origin for the $\tilde{A}^1B_{2u} \leftarrow \tilde{X}^1A_{1g}$ Transition of C_6H_6 Isolated in Solid H_2 of an Ortho/Para Ratio of: (a) 3:1; (b) 1:1.

In these investigations, radiation of wavelength shorter than 2200A. is filtered out to prevent excitations into higher singlet electronic states, but attempts were made to irradiate the film in this energy region for a few hours in search of further alterations in the relative line strengths of the fine structure. At lower temperatures than the boiling point of liquid nitrogen, the para-form of hydrogen predominates. A medium of predominantly para-hydrogen might be generated by the presence of a paramagnetic ortho/para conversion catalyst in solid hydrogen, such as the benzene impurity raised to its triplet state. The effect of a further reduction of the ortho/para ratio upon the benzene spectrum was sought but the resulting spectra were inconclusive, revealing no significant changes.

The signal from a more concentrated solution of benzene in solid hydrogen is also of interest. The benzene trap was cooled with a chloroform slush to a temperature of $-63.5^{\circ}C$. at which the benzene vapor pressure is $\sim 5 \times 10^{-2}$ mm. Hg. The resulting film was highly fragmented, however, and the illuminating continuum for the absorption study was almost totally scattered away from the spectrograph slit. Successful spectra under these conditions were not obtained.

SOME THOUGHTS FOR FUTURE CONSIDERATION

The extent of optical investigations into the benzene-solid hydrogen system presented in this report has elements that beg for further observation and analysis. The more demanding questions concern the changes in the line strengths of the fine structure exhibited by benzene isolated in solid hydrogen samples of varying ortho/para ratios and the shifts in position of the fine structure between solid hydrogen and deuterium mediums. But accounting for such features as the strength of the continuum underlying the fine structure or the presence of additional lines in the fine structure of perdeuterobenzene transitions or the difference in relative intensities of the components of the red doublet between hydrogen and deuterium systems is important.

Systems in which benzene or perdeuterobenzene is isolated in solid deuterium show a continuum much greater relative to the superimposed fine structure than that shown by the corresponding systems involving solid hydrogen (Figures 5-1 and 5-2). Some of the experimental details are perhaps pertinent. For instance, at a temperature of 2°K., the probability of lattice distortions being frozen into the sample is greater for deuterium than for hydrogen judging from the greater crystalline forces in deuterium

as reflected by its higher freezing point. As a result, the environments about isolated benzene molecules are more random in configuration and more uniform in frequency of occurrence with a consequent leveling effect upon the fine structure.

In addition, the 0.5% fraction of impurities in the source of deuterium will almost certainly result in lattice distortions plentiful enough to significantly broaden an otherwise sharp signal.

Of possible significance also is the difference in zero point effects between solid hydrogen and deuterium as illustrated in the smaller lattice cell cimensions of solid deuterium. The distortion caused by isolating a large molecule such as benzene in a light matrix may be more pronounced for a deuterium medium than for a medium of hydrogen. Reproducible benzene environments would be less frequent resulting in a broad signal.

Benzene isolated in solid hydrogen and solid deuterium exhibits vibronic transitions red-shifted with respect to the gas phase spectrum. The magnitude of these shifts as regards the reddest component of the fine structure is $\sim$115 cm^{-1} and $\sim$130 cm^{-1}, respectively, values reproduced in the perdeuterobenzene systems. It should also be noted that the red-shift observed for benzene isolated in solid argon is of similar magnitude (Table 5-1).

But if the benzene-hydrogen interaction is modelled from the (6-12) potential and the attractive term is derived from London dispersion energy formulations [7], it is predicted that the contribution of the attractive interaction to the shift is proportional to the polarizability of the solvent. The mean polarizability of hydrogen is about one half that of argon, suggesting that benzene in solid hydrogen would be expected to be blue-shifted relative to benzene in solid argon. Such an analysis is highly suspect, however, if for no other reason than other forms of interaction may be critical. Even though the nearest-neighbor distances in solid argon and in solid hydrogen are nearly the same, the van der Waals radius is larger for argon than for hydrogen [8]. Consequently benzene particles perhaps experience a more "squeezed" environment in argon than in hydrogen, resulting in a larger contribution to benzene shifts due to repulsive exchange interactions. The greater repulsive interaction experienced in solid argon will compensate somewhat for the postulated greater attraction between benzene and solid argon. Furthermore, no consideration of the interaction between quadrupole moments in benzene and hydrogen has been made. Because the moment for benzene is large, the contribution of this interaction is significant and it can be attractive. Since argon atoms possess no multipole

moments, such an interaction plays no part in benzene-argon systems, but in benzene-hydrogen systems it can make up for the different dispersion interactions between the two mediums.

The question arises concerning the shift in different directions of the fine structure in comparing the spectra of benzene in solid hydrogen with that of benzene in solid deuterium (Figure 5-1). The components between 38489 and 38604 cm^{-1} in the hydrogen medium are shifted to the blue by 14 cm^{-1} on the average in the deuterium environment wheras the red doublet is red-shifted by about 7 cm^{-1}. The mean value of the polarizabilities for hydrogen and deuterium differ, being smaller for the latter molecule. In addition, the lattice dimensions for deuterium are less than those for hydrogen. These two trends would be likely to shift the fine structure lines in the hydrogen medium to higher energy. This would account for the differences in line positions in the five-line pattern, if it is assumed that the fine structure can be attributed to environmental effects and, in particular, to multiple sites (to be discussed below). But with this assumption an additional feature must be considered for the structure that undergoes a red-shift from a hydrogen to a deuterium medium. Possible schemes that come to mind include situating benzene in a more spacious environment, such as a site with vacancies

neighboring the solute, in which a reduction in the distance between benzene and nearest neighbors that would occur from hydrogen to deuterium would result in a red-shift in the spectrum. In other words, the dependence on the intermolecular spacings of the attractive and repulsive contributions to shifts would enhance the attractive contribution over the repulsive in a deuterium system. Such defects would be more prevalent in a solid deuterium film deposited at $2^{\circ}K$. since stronger crystalline forces reduce the amount of annealing, which would correlate with the increased signal strength observed for the red doublet in a deuterium environment (Figure 5-1).

Another scheme accounts for the red structure with a model of resonance interactions between benzene molecules at non-nearest neighbor positions. The decrease of the distance between the resonance pair that would occur in a solid deuterium medium would possibly result in a greater attractive interaction with a resultant red shift in the spectrum. Such a model has been postulated for the lower energy component of the fine structure for benzene isolated in solid argon [9], which again points out the similarity in the fine structure of benzene spectra in different solvents. The fact that the members of the gross doublet structure of $\sim$100 cm^{-1} splitting in the benzene-hydrogen system undergo opposing shifts when the

solvent is changed to deuterium suggests significantly different environments at the source of the structure which in turn bears strongly upon the cause of similar doublet structure found in other mediums.

The sharpness of the lines is a possible indicator of the strength of the interactions between benzene and its hydrogenic environment. In solid hydrogen the lines are approximately 5 cm^{-1} wide at half intensity. Yet, as evidenced by the five-line multiplet pattern, the spread in the difference in solvent perturbation energies between ground and excited benzene states is 40 cm^{-1}, the spread of perturbation energies for each electronic state probably greater. In any case the sites responsible for each fine structure line must be well-defined. Such a situation is not immediately reasonable, however, as some lattice distortion with consequent signal broadening would be expected from inserting a large organic molecule into a light hydrogen matrix. Yet strong attractive interactions may produce a finite number of sharply defined environments.

Contributions to the attraction between benzene and hydrogen arise from London dispersion forces and interactions between quadrupole moments. At 3.75 A., the intermolecular distance in solid hydrogen, the magnitude of the dispersive attraction is of the order of 30 cm^{-1}. Preliminary calculations of the quadrupolar interaction between benzene and

hydrogen situated directly above the center of the pi-ring at the same intermolecular distance indicate that the interaction is attractive by ~ 30 cm^{-1} if the moment is averaged over the rotational motion of the $m=\pm 1$ substates of ortho-hydrogen. In the m=0 substate hydrogen is repulsed by the benzene moment. Para-hydrogen which exhibits no rotational motion undergoes an interaction whose sign depends upon the orientation of the hydrogen axis, but exhibits a maximum attraction nearly 200 cm^{-1} strong. The surprizing strength of these interactions is a result of the size of the benzene quadrupole moment, an order-of-magnitude greater than that for hydrogen.

The sharpness of the lines, the strength of the quadrupolar interactions, and the changes in line intensities that result from a change in the ortho/para ratio of the solid hydrogen medium suggest the existence of a well-defined complex of benzene and hydrogen molecules. As an example of a model which would result in the observed fine structure, matrix-isolated benzene is envisioned as interacting with four neighboring hydrogen molecules. The magnitude of each para interaction is dependent upon the ortho- or para-nature of the hydrogen molecule, but otherwise the interactions are equivalent, i.e. an ortho-hydrogen in any of the four neighboring positions experiences the same interaction. The total interaction depends

on the number of ortho- and para-molecules about the benzene. When the ortho/para ratio of the hydrogen source is reduced from 3:1 to 1:1, frequencies of finding a particular ratio about an isolated benzene molecule are expected to change as follows:

	ortho/para ratio of H_2 sample	
	3:1	1:1
4 o-H_2	81/256	16/256
3 o-H_2, 1 p-H_2	27/256	16/256
2 o-H_2, 2 p-H_2	9/256	16/256
1 o-H_2, 3 p-H_2	3/256	16/256
4 p-H_2	1/256	16/256

And the changes in the five-line spectral pattern can be viewed as reflecting these altered frequencies. For example, line 1 in Figure 5-4 corresponds to the situation of four ortho-hydrogen neighbors, whereas the increase of probability for the situation of four para-hydrogen neighbors would correspond to the intensity increase for line 5. Of course, any model will be required to stand up under a more exact evaluation of site interactions.

In defense of this type of complex as the nature of multiple sites giving rise to the spectral fine structure, only in a hydrogenic solvent medium has this type of fine

structure been observed. And in all of the mediums used to isolate benzene, hydrogen and deuterium appear to be the sole instances of a system with nuclear degrees-of-freedom and relatively unhindered rotational motion at very low temperatures. Hence, the interaction between benzene and a hydrogenic molecule can exhibit more than one strength as a result of rotational averaging, if the solvent molecule is found to exist in more than one rotational state at low temperatures.

REFERENCES

1. B. Meyer, Low Temperature Spectroscopy, American Elsevier, 1971.

2. V. R. Dietz, J. Am. Chem. Soc. 55, 472 (1933).

3. A. H. Singleton, Adv. Cryog. Eng. 13, 409 (1968).

4. M. Kasha, J. Opt. Soc. Am. 38, 929 (1948).

5. R. P. Frosch, Ph.D. Thesis, Calif. Inst. of Tech., 1965.

6. G. Herzberg, Electronic Spectra of Polyatomic Molecules, D. Van Nostrand, 1967.

7. G. W. Robinson, J. Molec. Spectrosc. 6, 58 (1961).

8 J. O. Hirschfelder, C. F. Curtiss, R. B. Bird, Molecular Theory of Gases and Liquids, J. Wiley and Sons, 1954.

9. G. Smith, S. Henry, C. E. Blount, J. Molec. Spectrosc. 35, 61 (1970)